Electronic Supplementary Material (ESI) for Dalton Transactions.

Supplementary Materials for

Highly phosphorescent organopalladium(II) complexes with metal-metal-to-ligand charge-transfer excited states in fluid solutions

Jinqiang Lin, Chao Zou, Xiaobao Zhang, Qin Gao, Sa Suo, Qihang Zhuo, Xiaoyong Chang, Mo Xie and Wei Lu*

Department of Chemistry, Southern University of Science and Technology, Shenzhen, Guangdong 518055, P. R. China.

E-mail: luw@sustech.edu.cn

Experimental Section

Materials. All reagents were purchased from commercial sources and used as received. The solvents used for synthesis were of analytical grade unless stated otherwise. The diacetylides and the precursor compounds [R-(C^N^N)PdCl] (R-HC^N^N = R-substituted 6-phenyl-2,2’-bipyridine) were prepared according to modified literature methods.[1-3]

Characterization. ^{1}H, ^{13}C, ^{19}F, NMR spectra were recorded with Bruker Avance 400 FT-NMR or 500 FT-NMR spectrometers. Infrared spectra were recorded on a Bruker V80 spectrometer. UV-Vis absorption spectra were recorded on a Thermo Scientific Evolution 201 UV-Visible Spectrophotometer. HR-MS (high resolution mass spectra) were obtained on a Thermo Scientific Q Exative mass spectrometer, operated in heated electrospray ionization (HESI) mode, coupled with Thermo Scientific Ultimate 3000 system. Photo-luminescent properties (solution and solid) were recorded via Edinburg spectrometer FLS-980 equipped with MCP-PMT and NIR-PMT detectors. Emission lifetime measurements were performed with Hamamatsu compact fluorescence lifetime spectrometer C11367. Absolute luminescent quantum yields were recorded with Hamamatsu absolute PL quantum yield spectrometer C11347. Time-resolved emission and transient absorption spectra were recorded with Edinburgh LP-920 Laser Flash Photolysis Spectrometer equipped with ICCD detector. The cyclic voltammetry was measured in N_2 saturated dichloromethane containing 0.10 M Bu_4NPF_6 as supporting electrolyte at 298 K; Pt electrode as counter electrode; glassy carbon electrode as working electrode and the Ag/AgCl couple as the reference electrode; Ferrocene (Fc) was used as the internal reference (scan rates: 50 mV/s).

Single crystals of **1** suitable for X-ray diffraction analysis were obtained by diffusion of diethyl ether into the dichloromethane solution. While crystals **2** ·Et_2O and **5** ·DMF were obtained by diffusion of diethyl ether into the DMF solution. Crystal **3** was gained by diffusion of diethyl ether into the chloroform solution. Crystal **5** ·DMSO was collected after cooling down a hot DMSO solution. The diffraction data were collected by a 'Bruker APEX-II CCD' diffractometer. The crystal was kept at 100 K during data collection. Using Olex2, the structure was solved with the XT structure solution program using Direct Methods and refined with the XL refinement package using Least Squares minimization.

Synthesis and characterization.

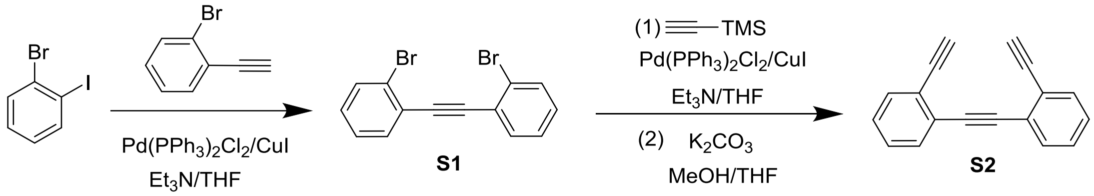

S1. This compound was prepared via the literature method with modifications. A mixture of 1-bromo-2-iodobenzene (2.83 g, 10 mmol), 1-bromo-2-ethynylbenzene (1.84 g, 10 mmol), $Pd(PPh_3)_2Cl_2$ (351 mg, 0.5 mmol) and CuI (191 mg, 1 mmol) were stirred in the mixture solvent Et_3N (25 mL)/ THF (5 mL) at 50 ^oC under N_2 overnight. The solvent was removed in vacuo and the pure product was gained as white powder after column chromatography using n-hexane as eluent. Yield 78%. ^1H NMR (500 MHz, $CDCl_3$) δ 7.71 – 7.52 (m, 4H), 7.30 (t, J = 7.5 Hz, 2H), 7.23 (t, J = 8.3 Hz, 2H).

S2. This compound was prepared via the literature method with modifications. A mixture of **S1** (334 mg, 1 mmol), ethynyltrimethylsilane (10 mmol, 1.4 mL), $Pd(PPh_3)_2Cl_2$ (70 mg, 0.1 mmol) and CuI (38 mg, 0.2 mmol) were stirred in the mixture solvent Et_3N (10 mL)/THF (3 mL) at 80 ^oC under N_2 for 24 hours. The solvent was removed in vacuo and the residue was dissolved in the MeOH/THF (1:5). K_2CO_3 (1.38 g, 10 mmol) was added to the solution and stirred at room temperature for 2 hours. The solid was filtered and the filtrate was evaporated in vacuo. pure product was gained as brown powder after column chromatography using *n*-hexane/ethylacetate as eluent. Yield 46%. ^1H NMR (400 MHz, $CDCl_3$) δ 7.68 – 7.56 (m, 2H), 7.57 – 7.44 (m, 2H), 7.42 – 7.27 (m, 4H), 3.34 (s, 2H).

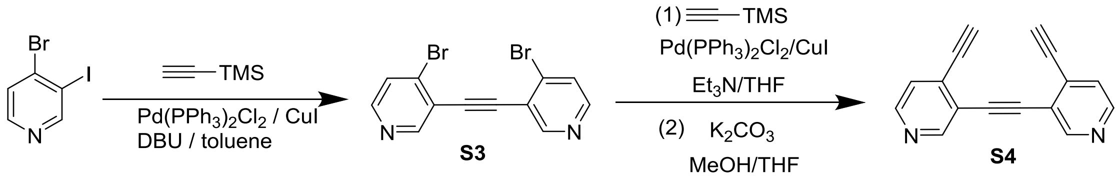

S3. This compound was prepared via the literature method with modifications. A mixture of 2-bromo-3-iodopyridine (2.28 g, 8 mmol), $Pd(PPh_3)_2Cl_2$ (168 mg, 0.48

mmol), CuI (152 mg, 0.8 mmol) and DBU (7.2 mL, 48 mmol) were dissolved in toluene (40 mL) under N_2. Then ethynyltrimethylsilane (0.4 mmol, 0.57 mL) and H_2O (0.06 mL) were added and the mixture was stirred at room temperature overnight. 50 mL ethylacetate was added to the mixture, then washed with brine and dried over anhydrous Na_2SO_4. The solvent was removed in vacuo and the pure product was given as white powder after column chromatography using n-hexane as eluent. Yield 61%. ^{1}H NMR (400 MHz, $CDCl_3$) δ 8.78 (s, 2H), 8.39 (s, 2H), 7.64 (d, J = 5.2 Hz, 2H). HR-MS (ESI): m/z = 338.8948, [M + H^+], calc. for [$C_{12}H_6Br_2N_2$ + H^+] m/z = 338.8956.

S4. The synthesis procedures were similar with those of **S2**. Yield 57%. ^{1}H NMR (500 MHz, $CDCl_3$) δ 8.82 (s, 2H), 8.55 (d, J = 5.1 Hz, 2H), 7.41 (d, J = 5.1 Hz, 2H), 3.58 (s, 2H). HR-MS (ESI): m/z = 229.0759, [M + H^+], calc. for [$C_{16}H_8N_2$ + H^+] m/z = 229.0766. IR: 2098 cm^{-1} ν(C≡C).

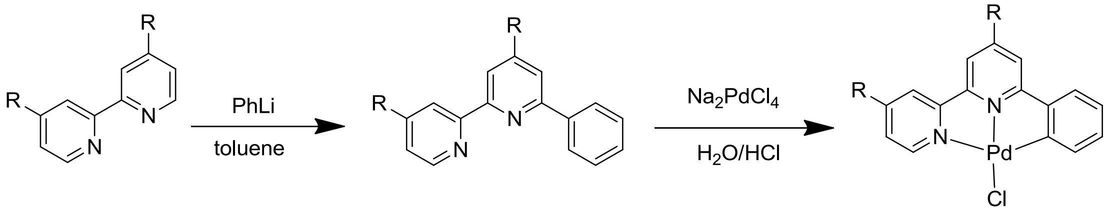

R = H **S5**
R = ^{t}Bu **S7**

R = H **S6**
R = ^{t}Bu **S8**

S5. This compound was prepared via the literature method with modifications. A solution of PhLi (22 mL, 22 mmol) in Et_2O was slowly added into the 50 mL toluene which contains 2,2'-bipyridine (3.12 g, 20 mmol). The mixture was refluxed overnight then cooled down to room temperature, filtered, the filtrate was rotated in vacuo to remove the solvent. The pure product was obtained after column chromatography using *n*-hexane/ethylacetate as eluent. Yield 32%. ^{1}H NMR (400 MHz, $CDCl_3$) δ 8.74 (d, J = 4.4 Hz, 1H), 8.69 (d, J = 8.0 Hz, 1H), 8.45(d, J = 7.8 Hz, 1H), 8.25–8.15 (m, 2H), 7.98–7.86 (m, 2H), 7.85–7.76 (m, 1H), 7.61–7.51 (m, 2H), 7.50–7.43 (m, 1H), 7.43–7.33 (m, 1H).

S6. Na_2PdCl_4 (882 mg, 3 mmol) and **S5** (696 mg, 3 mmol) were suspended in 40 mL water, then 3 mL concentrated hydrochloric acid was added. The mixture was heated to 95 °C and stirred overnight. yellowish green solid product was obtained by filtration, washed with H_2O, MeOH and Et_2O successively. Yield 88%. ^{1}H NMR (400 MHz, DMSO) δ 8.66 (d, J = 4.2 Hz, 1H), 8.53 (d, J = 8.0 Hz, 1H), 8.33 – 8.23 (m, 2H), 8.19 (t, J = 7.9 Hz, 1H), 8.10 – 7.99 (m, 1H), 7.81 (ddd, J = 7.6, 5.2, 1.1 Hz, 1H), 7.67 (dd, J = 7.2, 2.0 Hz, 1H), 7.54 (dd, J = 7.0, 1.8 Hz, 1H), 7.17 – 7.04 (m, 2H).

S7. The synthesis procedures were similar with those of **S5** except that 4,4'-di-*tert*-butyl-2,2'-bipyridine was used as the starting material. Yield 35%. ^{1}H NMR (500 MHz, $CDCl_3$) δ 8.90 (t, J = 14.8 Hz, 2H), 8.80 (t, J = 7.0 Hz, 1H), 8.18 – 8.11 (m, 2H), 7.90 (s, 1H), 7.70 (s, 1H), 7.57 (t, J = 7.5 Hz, 2H), 7.50 (t, J = 7.3 Hz, 1H), 1.53 (d, J = 2.9 Hz, 9H), 1.50 (d, J = 3.3 Hz, 9H).

S8. The synthesis procedures were similar with those of **S6** except that **S7** was used as the cyclometalated ligand. Yield 85%. ^{1}H NMR (400 MHz, $CDCl_3$) δ 8.76 (d, J = 5.6 Hz, 1H), 7.85 (d, J = 1.5 Hz, 1H), 7.79 (dd, J = 7.4, 1.4 Hz, 1H), 7.57 (dd, J = 7.2, 1.4 Hz, 2H), 7.48 (dd, J = 5.6, 1.8 Hz, 1H), 7.38 (dd, J = 7.4, 1.6 Hz, 1H), 7.09 (dtd, J = 18.7, 7.3, 1.4 Hz, 2H), 1.46 (s, 9H), 1.43 (s, 9H). HR-MS (ESI): m/z = 490.1473, [M – Cl + CH_3CN], calc. for [$C_{24}H_{27}N_2Pd$ – Cl + CH_3CN] m/z = 490.1475.

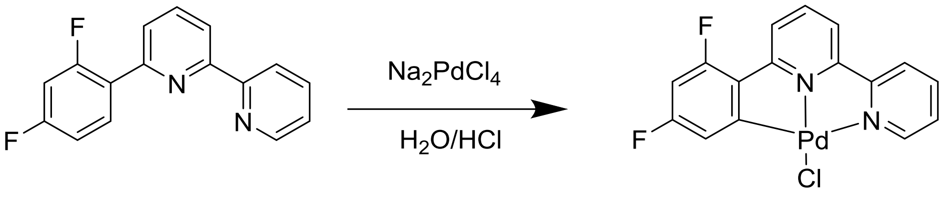

S9 **S10**

S10. The synthesis procedures were similar with those of **S6** except that **S9** was used as the cyclometalated ligand. Yield 85%. ^{1}H NMR (500 MHz, DMSO) δ 8.58 (d, *J* = 4.2 Hz, 1H), 8.50 (d, *J* = 8.0 Hz, 1H), 8.28 (dt, *J* = 7.8, 3.0 Hz, 2H), 8.19 (t, *J* = 8.0 Hz, 1H), 7.86 (d, *J* = 7.9 Hz, 1H), 7.83 – 7.74 (m, 1H), 7.06 (dd, *J* = 7.9, 2.4 Hz, 1H), 6.97 (s, 1H). ^{19}F NMR (376 MHz, DMSO) δ -105.75 (d, *J* = 8.9 Hz), -109.76 (d, *J* = 8.9 Hz). HR-MS (ESI): m/z = 414.0027, [M – Cl + CH_3CN], calc. for [$C_{16}H_9F_2N_2Pd$ – Cl + CH_3CN] m/z = 414.0034.

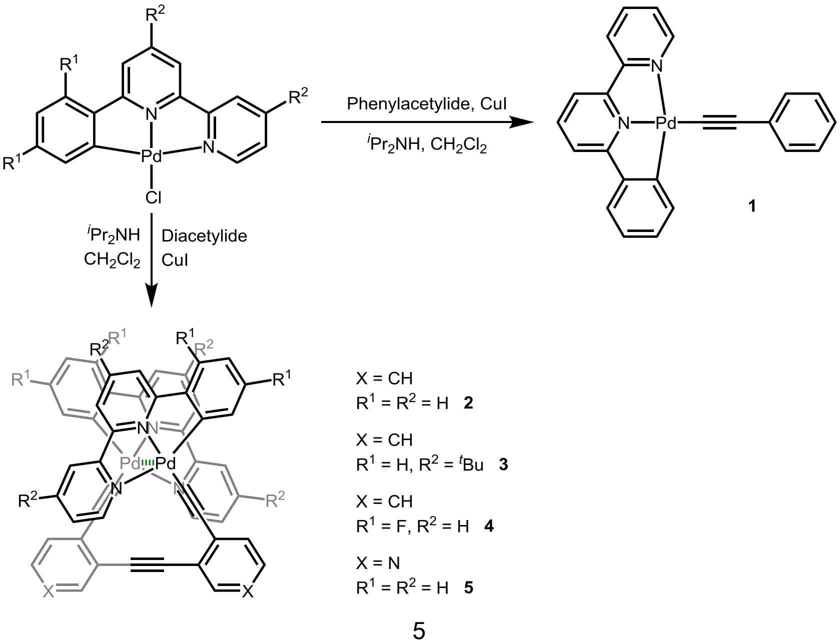

Complex 1. S6 (37 mg, 0.1 mmol) and CuI (ca. 1 mg) were suspended in 8 mL dichloromethane under N_2, then phenylacetylide (12 mg, 0.12 mmol) and diisopropylamine (2.5 mL) was added. The mixture was stirred at room temperature overnight, then rotated in vacuo to remove the solvent. The residue was washed with MeOH, Et_2O, and recrystallized from dichloromethane and Et_2O to give the pure product as a yellow solid. Yield 61%. ^{1}H NMR (500 MHz, CD_2Cl_2) δ 8.85 (d, J = 5.0 Hz, 1H), 7.95 (d, J = 3.7 Hz, 2H), 7.89 (d, J = 7.3 Hz, 1H), 7.83 (t, J = 8.0 Hz, 1H), 7.66 (d, J = 7.9 Hz, 1H), 7.56 (d, J = 8.0 Hz, 1H), 7.53 – 7.45 (m, 3H), 7.43 (d, J = 7.5 Hz, 1H), 7.28 (t, J = 7.6 Hz, 2H), 7.17 (t, J = 7.4 Hz, 1H), 7.12 (td, J = 7.3, 1.3 Hz, 1H), 7.10 – 7.03 (m, 1H). ^{13}C NMR (126 MHz, CD_2Cl_2) δ 163.37, 156.43, 155.61, 153.15, 151.80, 148.47, 140.13, 139.17, 139.06, 131.28, 130.36, 128.65, 127.98, 126.73, 125.07, 124.19, 124.16, 122.09, 118.86, 118.20, 115.42, 104.40. HR-MS (ESI): m/z = 421.0236, [M + Na^+], calc. for [$C_{24}H_{16}N_2Pd + Na^+$] m/z = 461.0250. IR: 2102 cm^{-1} ν(C≡C).

Complex 2. S2 (bridging ligand, 23 mg, 0.1 mmol), **S6** (precursor, 74 mg, 0.2 mmol) and CuI (ca. 1 mg) were suspended in 10 mL dichloromethane under N_2, then 3 mL diisopropylamine was added. The mixture was stirred at room temperature overnight, then rotated in vacuo to remove the solvent. The residue was washed with MeOH, Et_2O, and recrystallized from dichloromethane and Et_2O to give the pure product as an orange solid. Yield 74%. ^{1}H NMR (400 MHz, DMSO) δ 9.15 (d, J = 4.1 Hz, 2H), 8.12 (d, J = 8.1 Hz, 2H), 7.98 (td, J = 7.8, 1.6 Hz, 2H), 7.87 (t, J = 7.9 Hz, 2H), 7.75 (d, J = 7.8 Hz, 2H), 7.69 (d, J = 8.0 Hz, 2H), 7.57 (d, J = 7.3 Hz, 2H), 7.40 (d, J = 6.5 Hz, 2H), 7.31 (ddd, J = 16.0, 11.0, 4.4 Hz, 6H), 7.22 – 7.11 (m, 2H), 6.99 (dd, J = 6.7, 5.3 Hz, 2H), 6.94 – 6.86 (m, 2H), 6.81 (dd, J = 7.3, 6.1 Hz, 2H). HR-MS (ESI): m/z = 901.06264, [M + H^+], calc. for [$C_{50}H_{30}N_4Pd_2 + H^+$] m/z = 901.06225. IR: 2089 cm^{-1} ν(C≡C).

Complex 3. The synthesis procedures were similar with those of complex **2** except that **S8** was used as the precursor. Yield 51%. ^{1}H NMR (500 MHz, $CDCl_3$) δ 9.44 (d, J = 5.5 Hz, 2H), 7.63 (d, J = 7.4 Hz, 2H), 7.35 (d, J = 6.9 Hz, 4H), 7.19 (t, J = 7.0 Hz, 2H), 7.14 (t, J = 7.0 Hz, 4H), 7.10 (s, 2H), 6.96 – 6.86 (m, 4H), 6.80 (ddd, J = 17.8, 10.3, 6.5 Hz, 4H), 6.63 (d, J = 4.1 Hz, 2H), 1.39 (s, 18H), 1.33 (s, 18H). ^{13}C NMR (126 MHz, $CDCl_3$) δ 161.71, 161.41, 160.61, 158.38, 155.70, 155.18, 154.01, 148.21, 139.59, 132.44, 132.33, 131.40, 128.71, 127.38, 126.81, 125.78, 124.23, 122.69, 122.64, 122.50, 118.05, 114.27, 113.57, 102.84, 92.88, 35.52, 35.04, 30.66, 30.35. HR-MS (ESI): m/z = 1125.31363, [M + H^+], calc. for [$C_{66}H_{62}N_4Pd_2 + H^+$] m/z = 1125.31265. IR:2095 cm^{-1} ν(C≡C).

Complex 4. The synthesis procedures were similar to those of complex **2** except that **S10** was used as the precursor. Complex **4** is poorly soluble in common organic solvents. Yield 62%. ^{1}H NMR (400 MHz, DMSO) δ 9.27 (d, J = 5.3 Hz, 2H), 8.08 (d, J = 7.8 Hz, 2H), 7.95 (dd, J = 18.0, 8.6 Hz, 2H), 7.93 – 7.79 (m, 2H), 7.77 (d, J = 8.0 Hz, 2H), 7.60 (d, J = 7.4 Hz, 2H), 7.52 (d, J = 8.1 Hz, 2H), 7.41 – 7.27 (m, 2H), 7.27 – 7.16 (m, 2H), 7.14 (d, J = 7.6 Hz, 2H), 6.82 – 6.40 (m, 6H). ^{19}F NMR (376 MHz, DMSO) δ -106.59, -110.02. HR-MS (ESI): m/z = 973.02494, [M + H$^+$], calc. for [$C_{50}H_{26}F_4N_4Pd_2$ + H$^+$] m/z = 973.02459. IR: 2098 cm^{-1} ν(C≡C).

Complex 5. The synthesis procedures were similar with those of complex **2** except that **S4** was used as the bridging ligand. Yield 70%. ^{1}H NMR (500 MHz, DMSO) δ 9.12 (d, J = 4.7 Hz, 2H), 8.74 (s, 2H), 8.39 (d, J = 5.1 Hz, 2H), 8.03 (d, J = 7.8 Hz, 2H), 8.00 – 7.94 (m, 2H), 7.79 (t, J = 7.9 Hz, 2H), 7.59 (d, J = 8.0 Hz, 4H), 7.24 (d, J = 7.5 Hz, 2H), 7.16 (d, J = 5.2 Hz, 2H), 7.12 (d, J = 7.2 Hz, 2H), 7.04 – 6.96 (m, 2H), 6.88 (t, J = 7.4 Hz, 2H), 6.76 (t, J = 7.4 Hz, 2H). HR-MS (ESI): m/z = 903.05297, [M + H$^+$], calc. for [$C_{48}H_{28}N_6Pd_2$ + H$^+$] m/z = 903.05275. IR: 2090 cm^{-1} ν(C≡C).

Table S1. Crystal Data for **1**, **2**·DMSO, **3** and **5**·DMF.

	1	**2**·DMSO	**3**	**5**·DMF
formula	$C_{24}H_{16}N_2Pd$	$C_{52}H_{37}N_4OPd_2S$	$C_{66}H_{62}N_4Pd_2$	$C_{51}H_{35}N_7OPd_2$
fw	438.79	978.71	1123.99	974.66
colour	yellow	orange	orange	orange
crystal size	0.4×0.36×0.04	0.21×0.21×0.18	0.45×0.08×0.08	0.42×0.28×0.19
crystal system	monoclinic	orthorhombic	triclinic	orthorhombic
space group	$P2_1/n$	$P2_12_12_1$	P-1	$P2_12_12_1$
a, Å	11.6530(8)	11.4577(12)	14.9357(9)	11.9009(4)
b, Å	11.6528(7)	16.1072(19)	15.1568(9)	15.3904(6)
c, Å	14.4457(10)	22.226(2)	15.5763(9)	22.0285(9)
α, deg	90	90	118.321(2)	90
β, deg	108.836(2)	90	102.924(2)	90
γ, deg	90	90	105.600(2)	90
V, Å^3	1856.5(2)	4101.8(7)	2721.1(3)	4034.7(3)
Z	4	4	2	4
D_c, g cm^{-3}	1.570	1.585	1.372	1.605
μ, mm^{-1}	1.009	0.974	0.705	0.942
$F(000)$	880.0	1972.0	1156.0	1960.0
$2\theta_{max}$, deg	54.994	52.812	55.326	55.046
no. reflections	25272	32623	46175	39116
no. independent reflections	4253 [R(int) = 0.1021]	8394 [R(int) = 0.0716]	12632 [R(int) = 0.1049]	9260 [R(int) = 0.0300]
no. variables	244	543	661	553
GOF on F^2	1.051	1.029	1.063	0.942
$R_1{}^a$ [I>2σ(I)]	0.0330	0.0381	0.0670	0.0194
$wR_2{}^b$	0.0772	0.0586	0.1687	0.0497
residual ρ, eÅ^{-3}	+1.03, –0.86	+ 0.41, –0.43	+2.83, -1.66	+0.26, -0.33

^{a} $R = \Sigma||F_o|-|F_c||/\Sigma|F_o|$. ^{b} $Rw = \{\Sigma[w(F_o^2-F_c^2)^2]/\Sigma[w(F_o^2)^2]\}^{1/2}$

Table S2. Photophysical and electrochemical data of **1**–**5**. The $E_{0\text{-}0}$ energy was estimated from the onset of the emission bands of the complexes (476 nm for **1**; 550 nm for **2**–**5**).

	Medium	T / K	λ_{max} / nm	τ / µs	ϕ / %	k_r / s^{-1}	k_{nr} / s^{-1}	$E_{0\text{-}0}$ / eV	E_{pa} / V	E_{red} / V	$E^*_{(M^*/M^-)}$ / V	$E^*_{(M^+/M^*)}$ / V
1	Solid-state	298	560	3.1	3							
	Solid-state	77	515	35.3								
	CH_2Cl_2	298	-------					2.61	0.33	−1.90	0.71	−2.28
	MeTHF	77	476	52.0								
2	Solid-state	298	640	2.1	56							
	Solid-state	77	650	14.4								
	CH_2Cl_2	298	653	1.2	20	1.7×10^5	6.7×10^5	2.25	0.16	−1.95	0.30	−2.09
	MeTHF	77	477 648	49.1 11.8								
3	Solid-state	298	604	2.4	79							
	Solid-state	77	628	13.0								
	Toluene	298	655	2.0	48	2.4×10^5	2.6×10^5					
	MeTHF	298	645	0.96	12	1.3×10^5	9.2×10^5					
	CH_2Cl_2	298	630	2.5	46	1.8×10^5	2.2×10^5	2.25	0.29	−2.04	0.21	−1.96
	$CHCl_3$	298	633	2.7	42	1.6×10^5	2.1×10^5					
	acetone	298	628	2.5	36	1.4×10^5	2.6×10^5					
	CH_3CN	298	623	1.9	22	1.2×10^5	4.1×10^5					
	DMF	298	622	0.89	9	1.0×10^5	10.2×10^5					
	MeTHF	77	475 609	60.7 10.6								
4	Solid-state	298	622	1.5	19							
	Solid-state	77	650	12.7								
	CH_2Cl_2	298	635	2.0	30	1.5×10^5	3.5×10^5	-------	-------	-------	-------	-------
	MeTHF	77	501 630	1085.4 14.5								
5	Solid-state	298	622	1.9	27							
	Solid-state	77	630	12.8								
	CH_2Cl_2	298	640	1.9	30	1.6×10^5	3.7×10^5	2.25	0.37	−1.92	0.33	−1.88
	MeTHF	77	475 633	68.5 14.6								

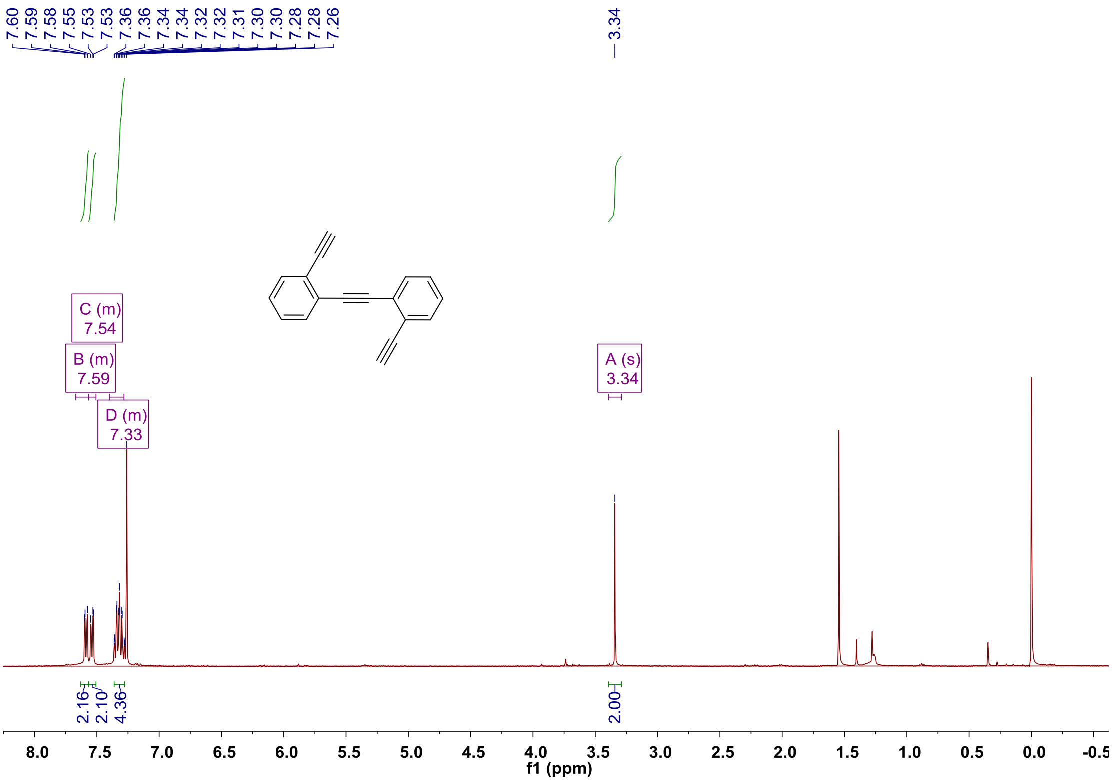

Figure S1. ^{1}H-NMR spectrum of **S2** in $CDCl_3$.

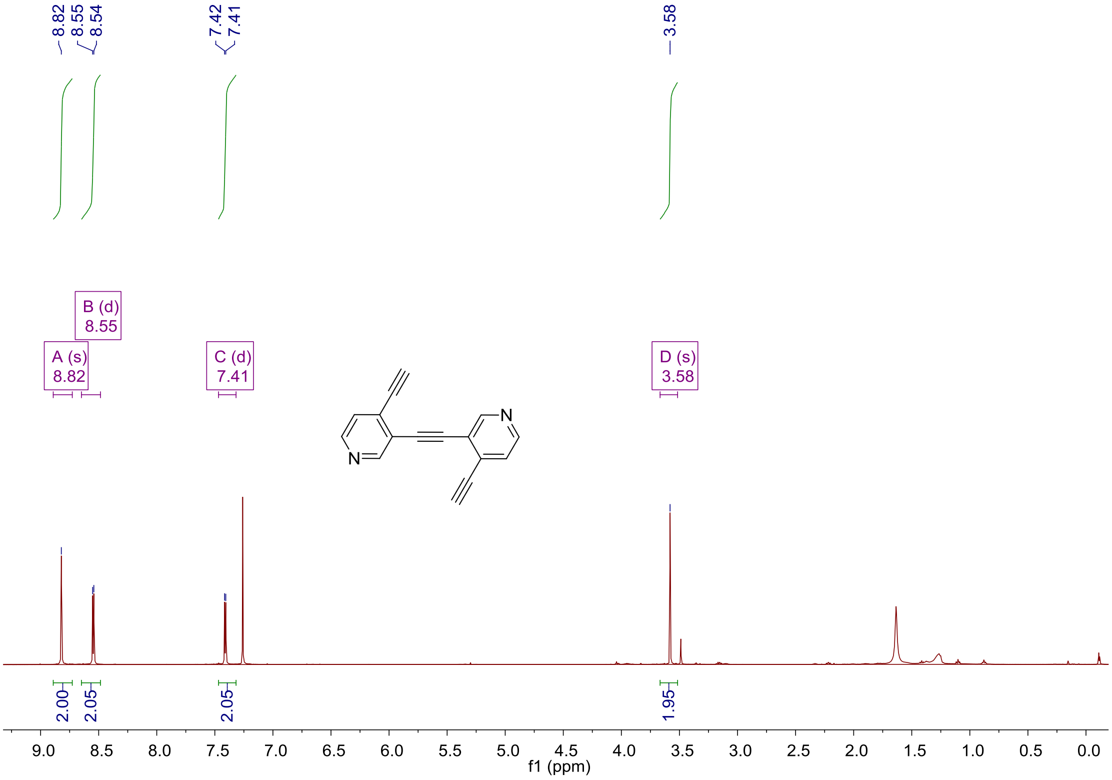

Figure S2. ^{1}H-NMR spectrum of **S4** in $CDCl_3$.

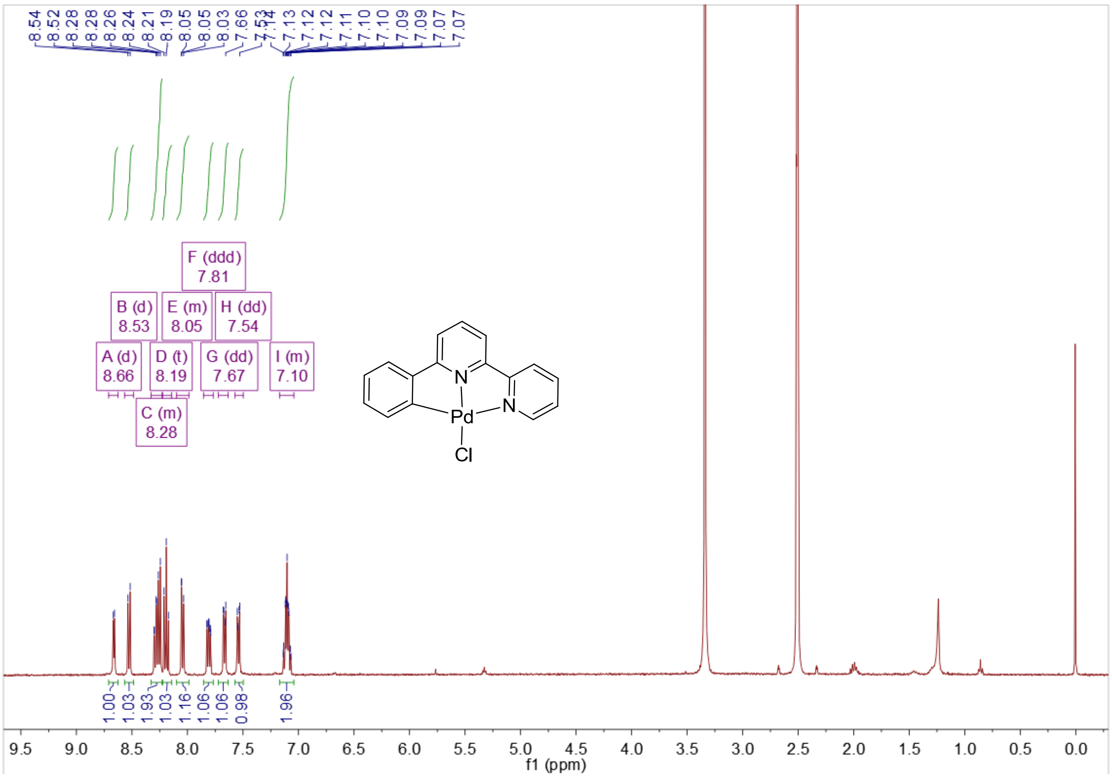

Figure S3. ^{1}H-NMR spectrum of **S6** in CDCl$_3$.

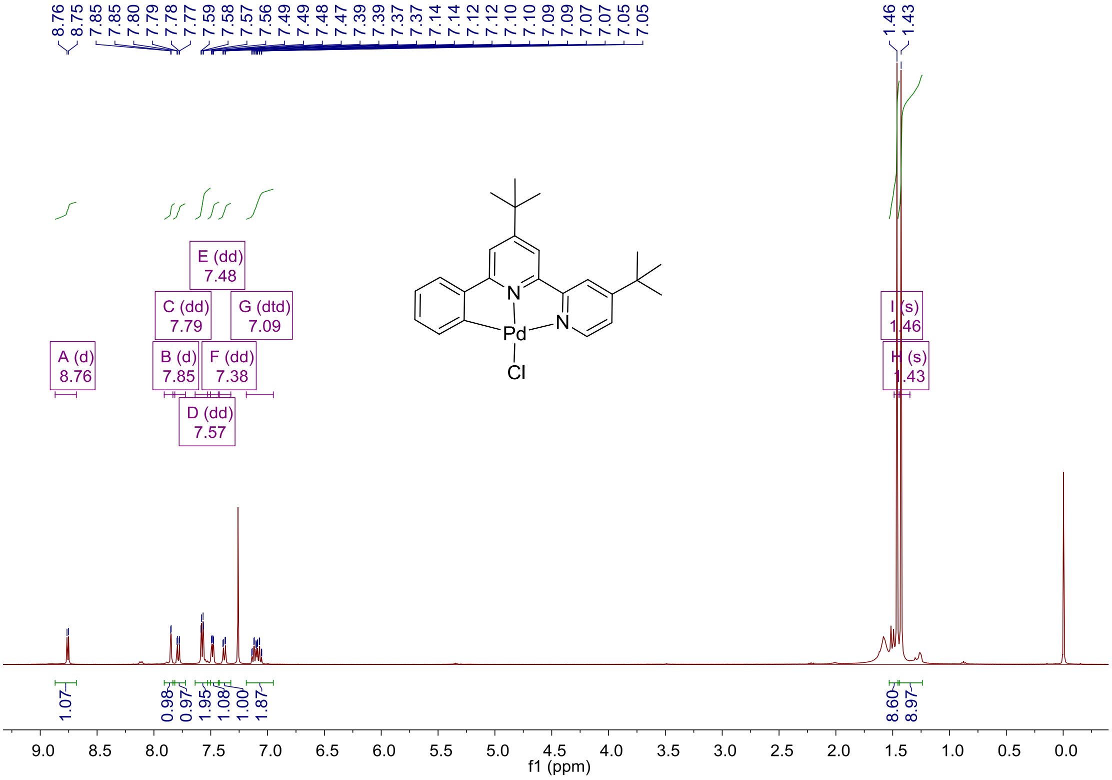

Figure S4. ^{1}H-NMR spectrum of **S8** in CDCl$_3$.

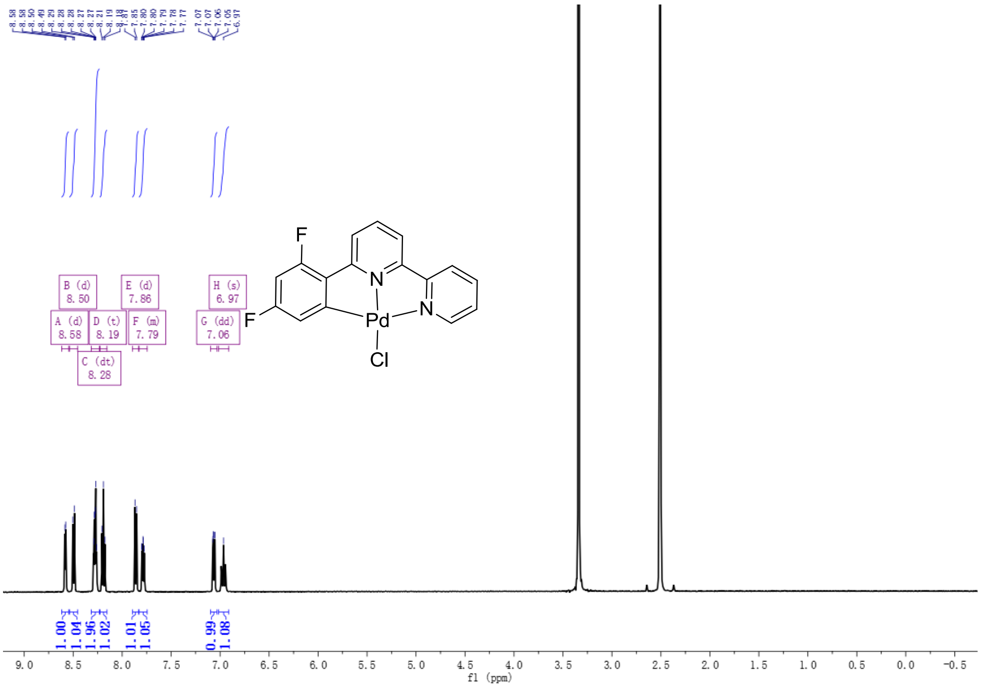

Figure S5. ^{1}H-NMR spectrum of **S10** in DMSO.

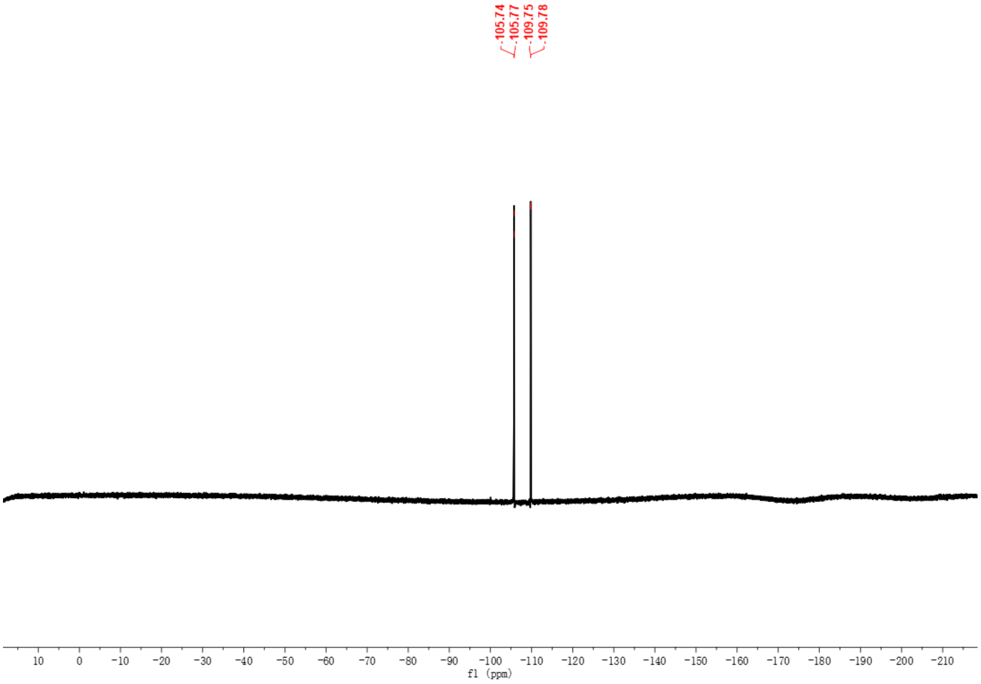

Figure S6. ^{19}F-NMR spectrum of **S10** in DMSO.

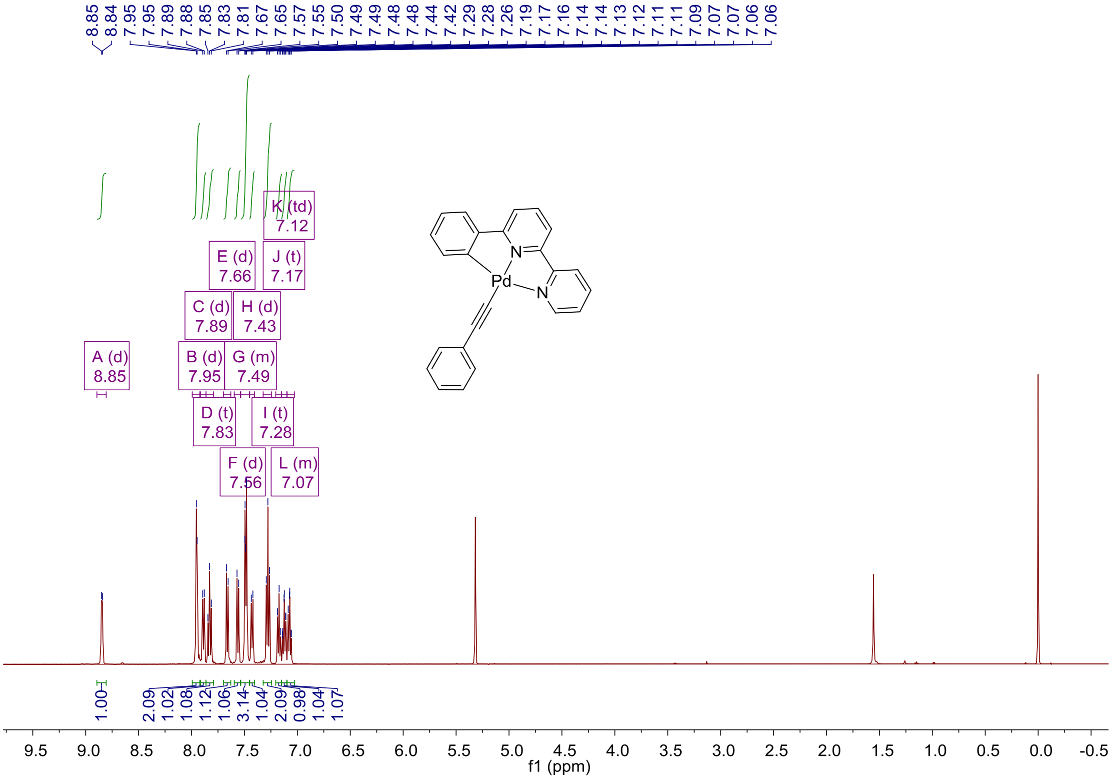

Figure S7. ^{1}H-NMR spectrum of **1** in CD_2Cl_2.

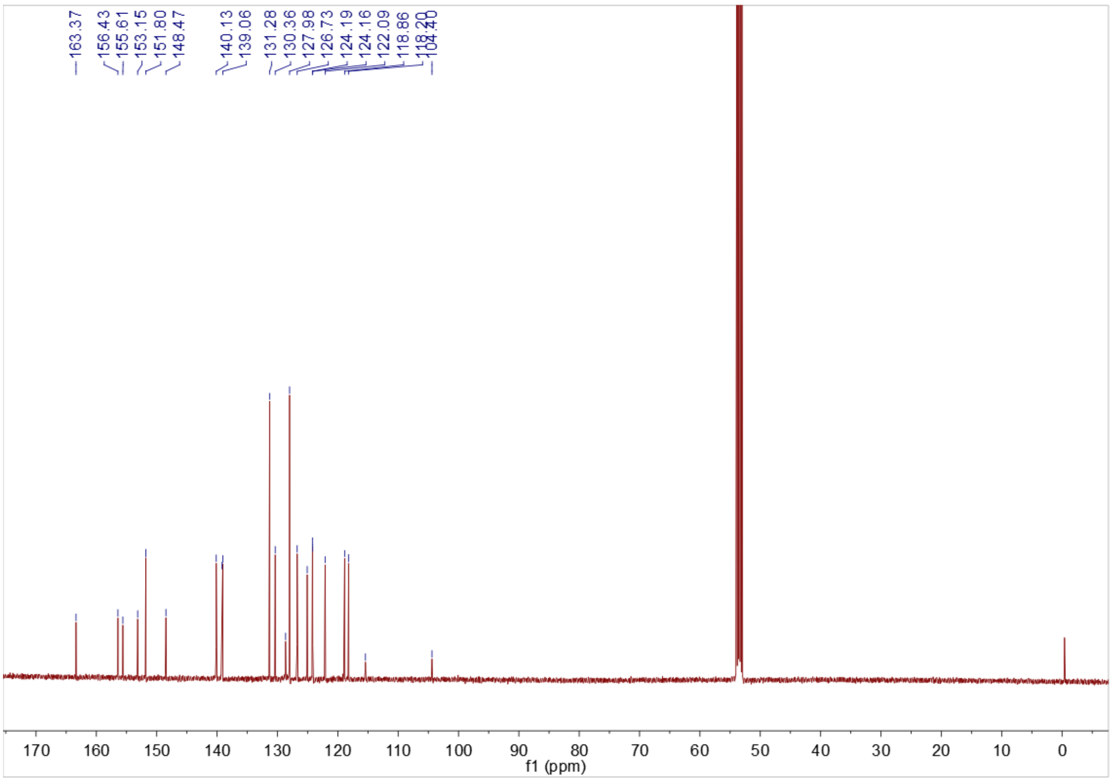

Figure S8. ^{13}C-NMR spectrum of **1** in CD_2Cl_2.

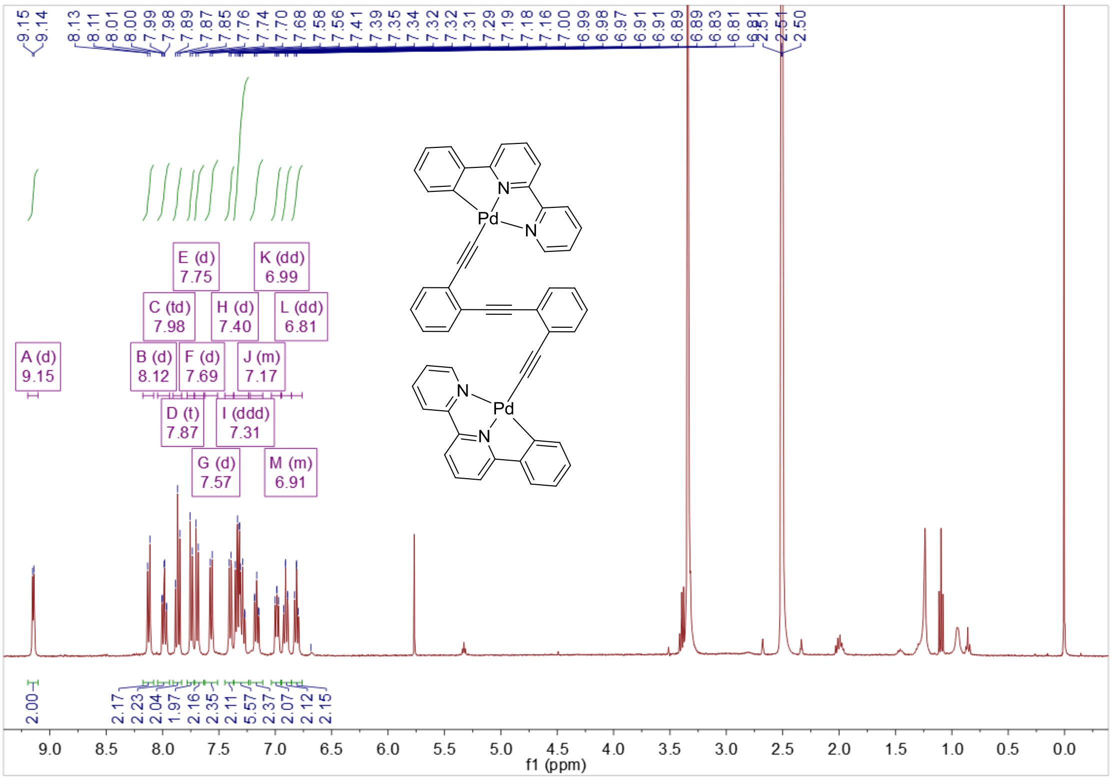

Figure S9. ^{1}H-NMR spectrum of **2** in DMSO.

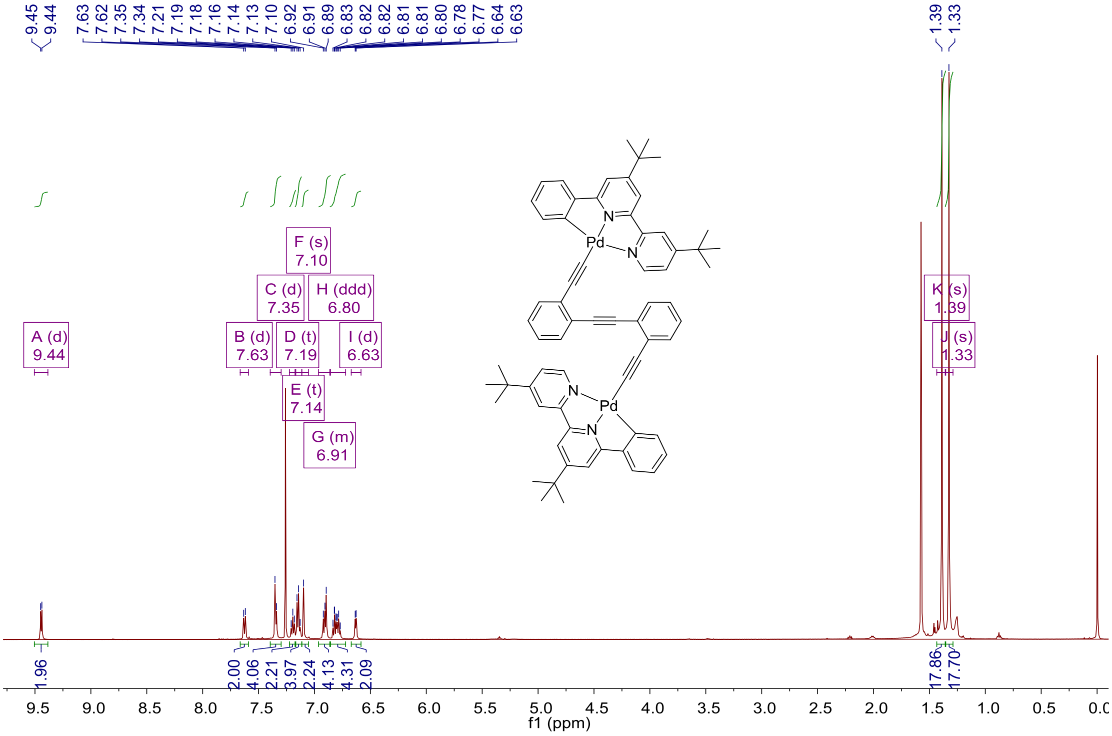

Figure S10. ^{1}H-NMR spectrum of **3** in $CDCl_3$.

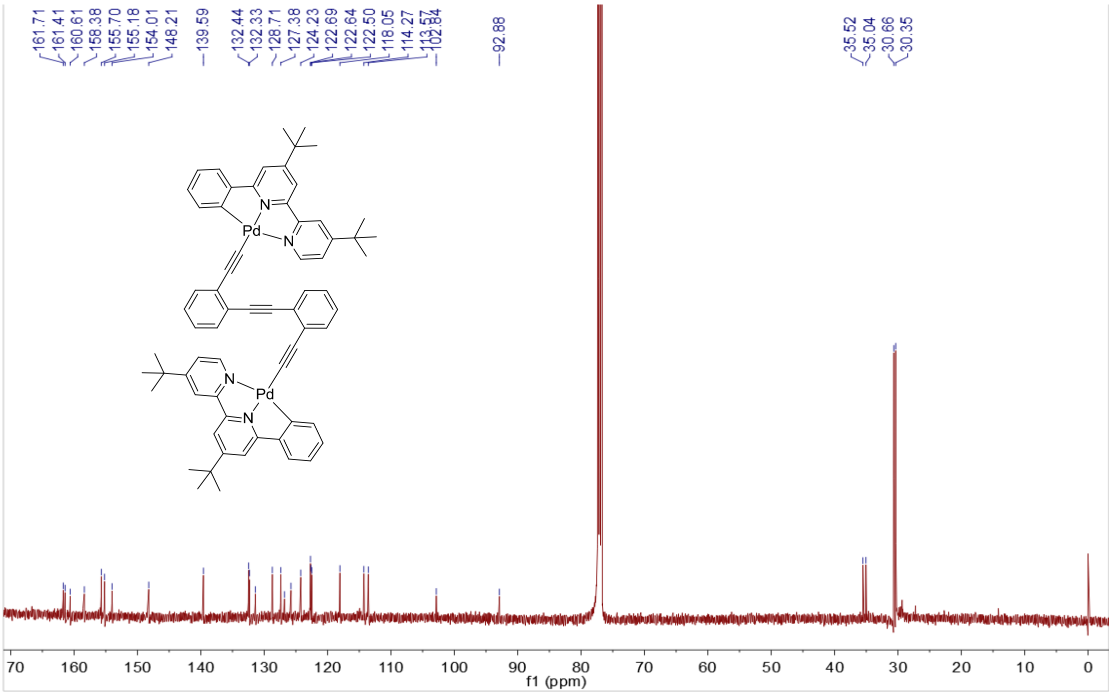

Figure S11. ^{13}C-NMR spectrum of **3** in $CDCl_3$.

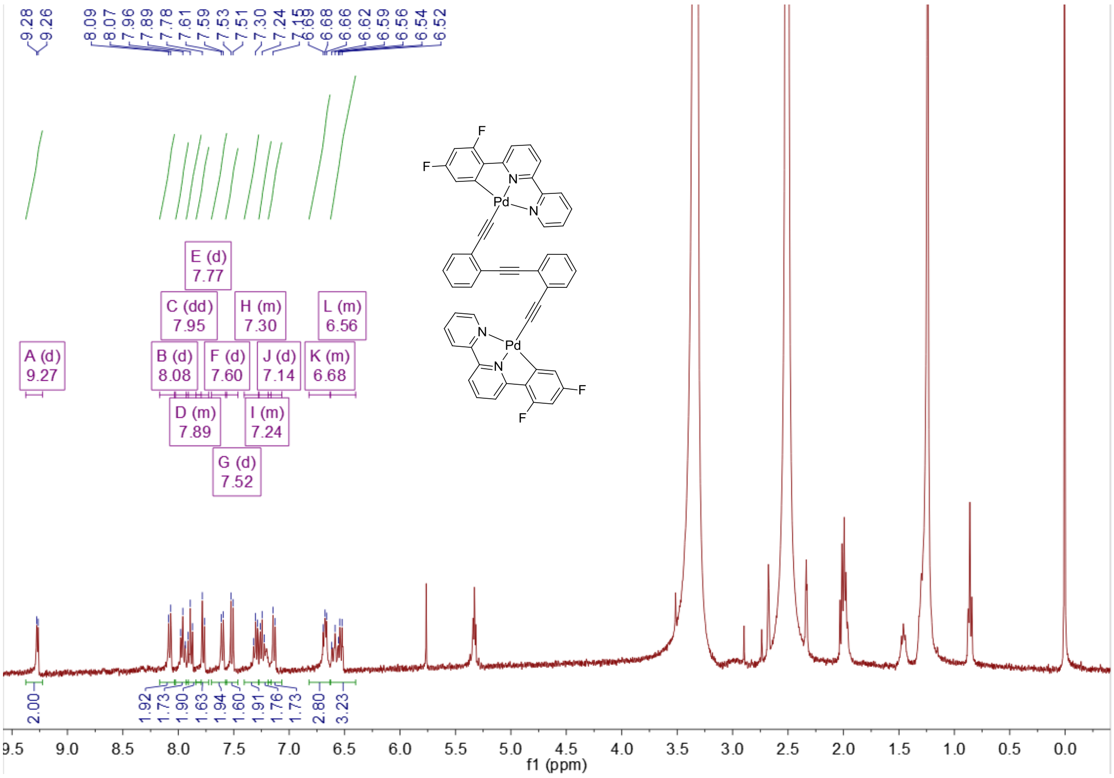

Figure S12. ^{1}H-NMR spectrum of **4** in DMSO.

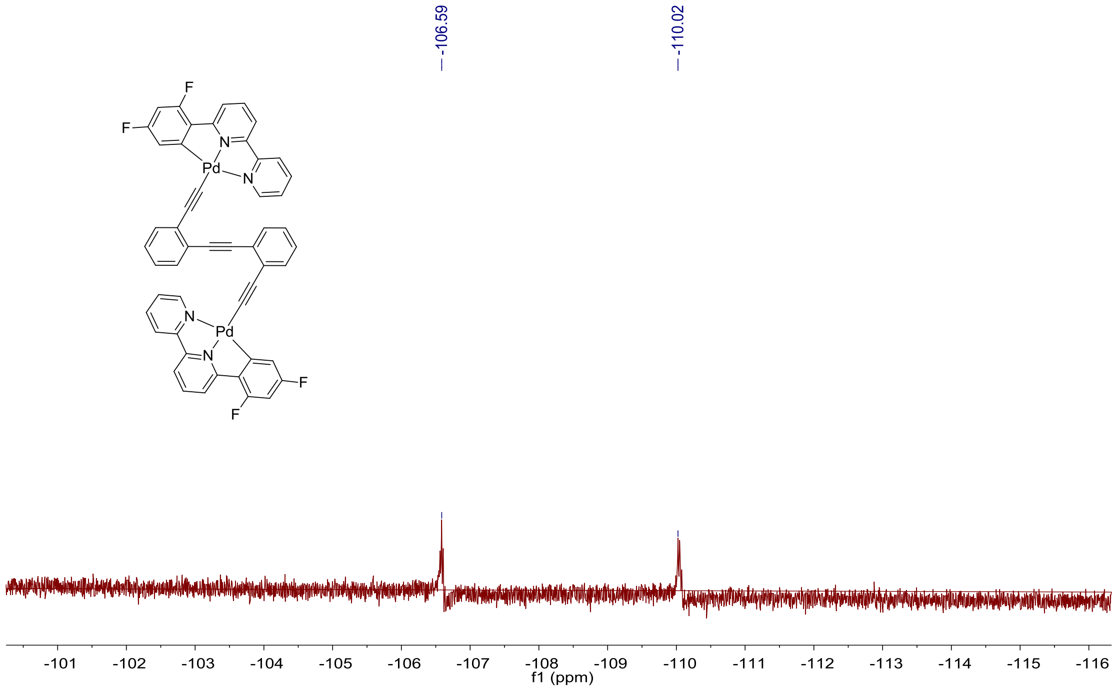

Figure S13. ^{19}F-NMR spectrum of **4** in DMSO.

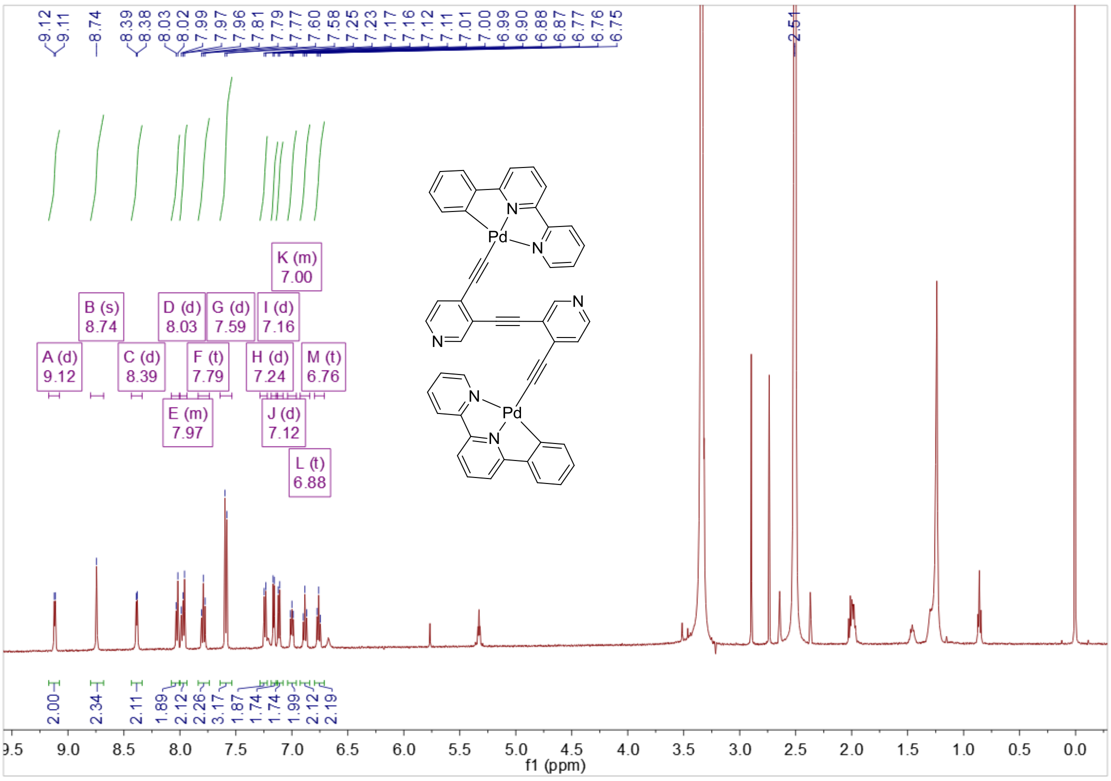

Figure S14. ^{1}H-NMR spectrum of **5** in DMSO.

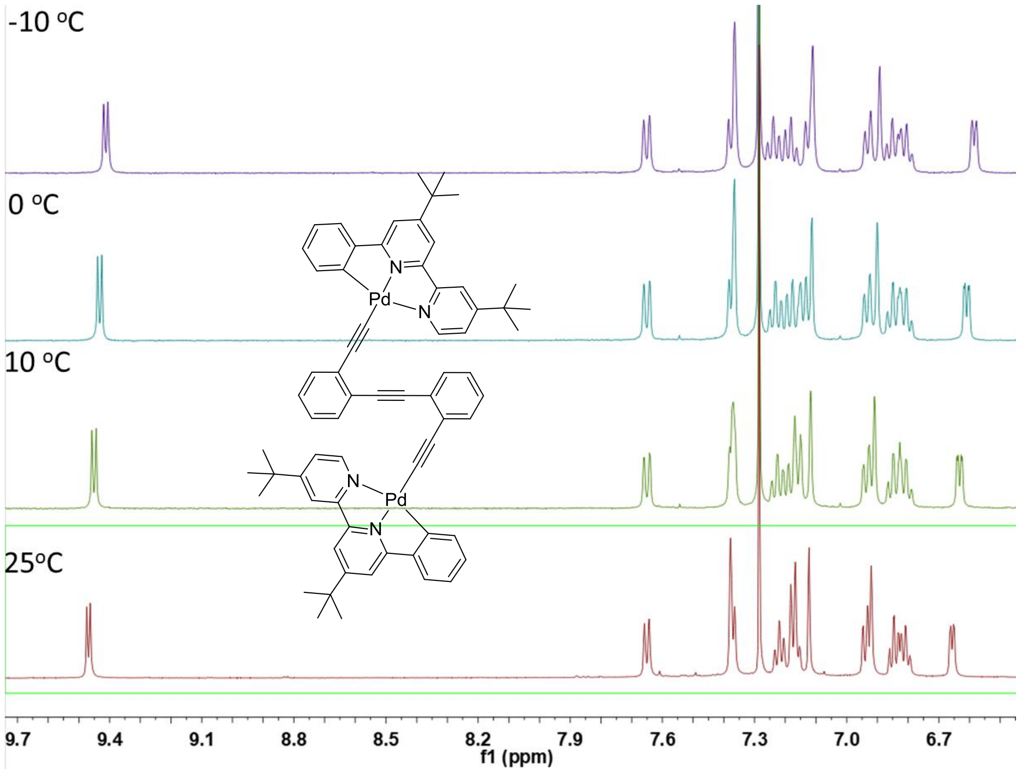

Figure S15. Varied temperature ^{1}H-NMR spectra of **3** in CDCl$_3$.

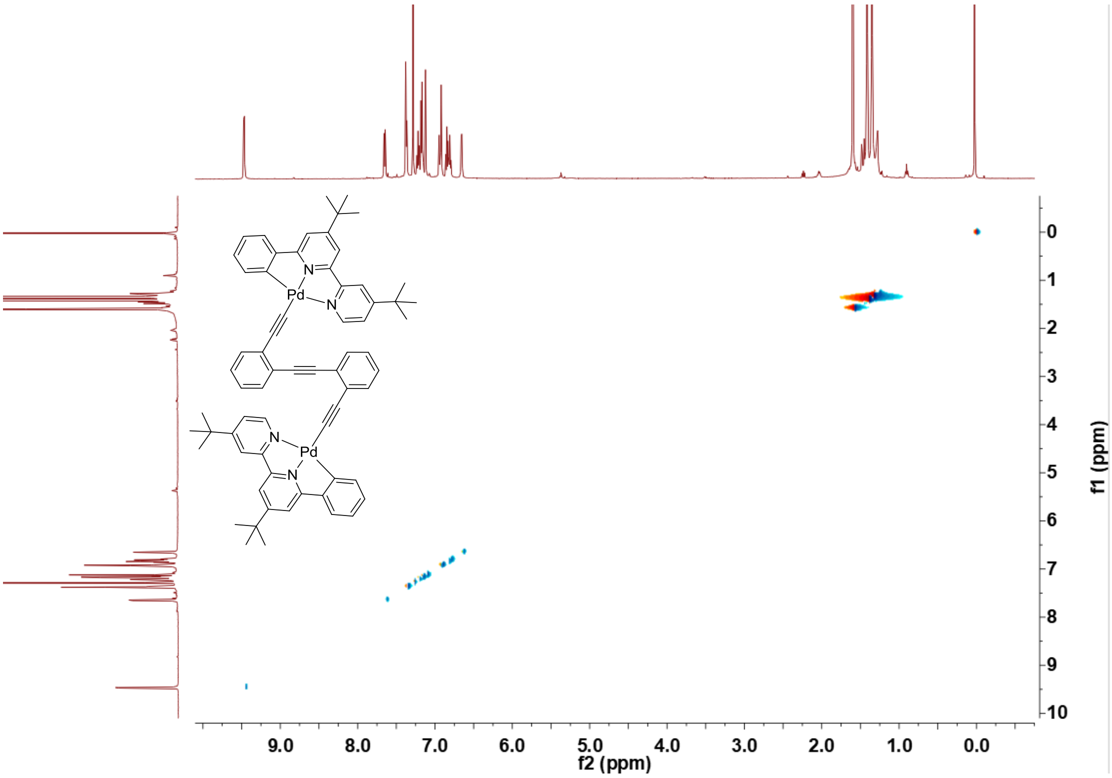

Figure S16. The NOESY spectrum of **3** in CDCl$_3$.

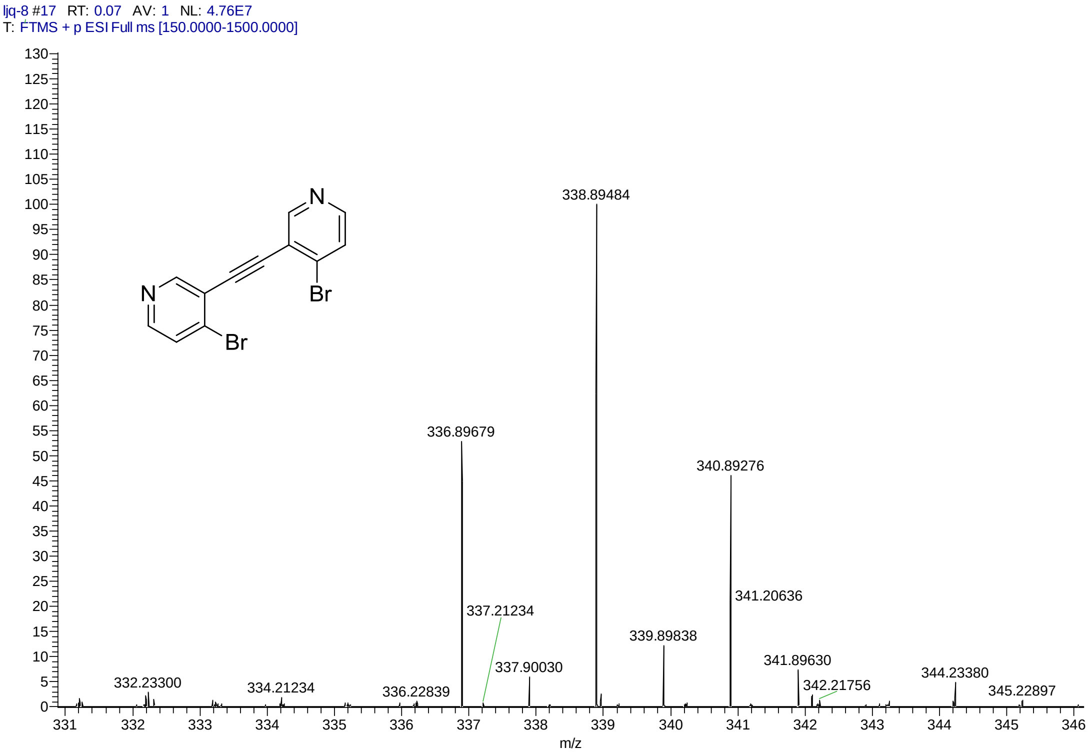

Figure S17. The HR-MS spectrum of **S3**.

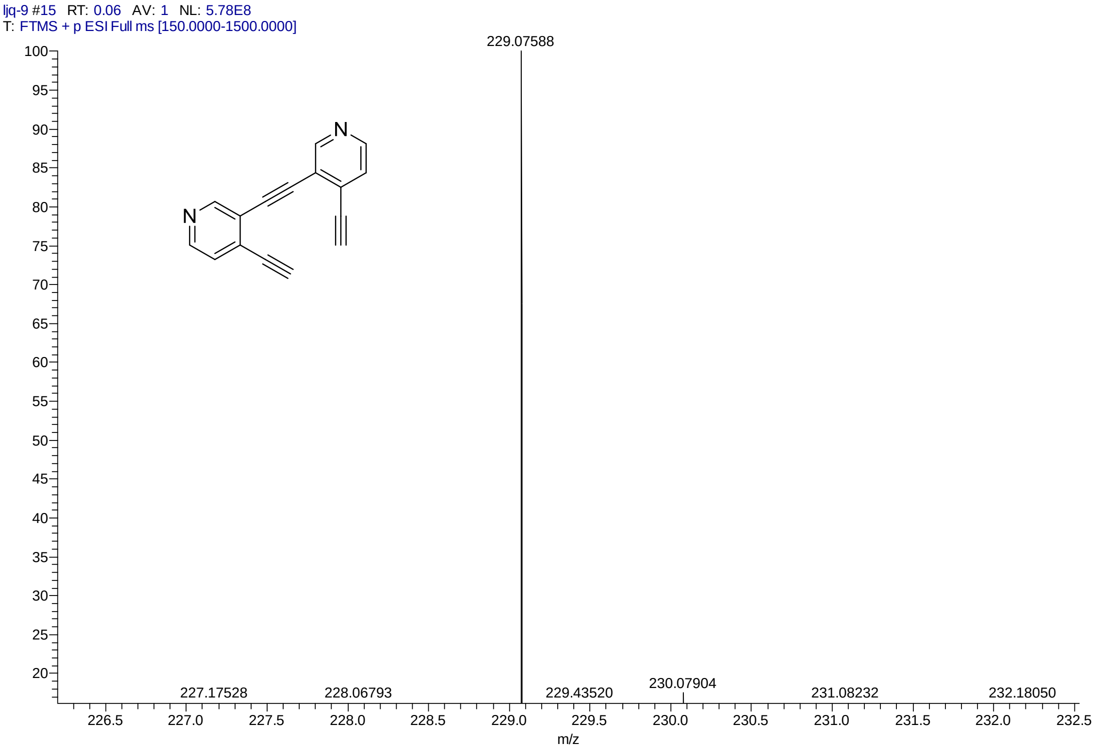

Figure S18. The HR-MS spectrum of **S4**.

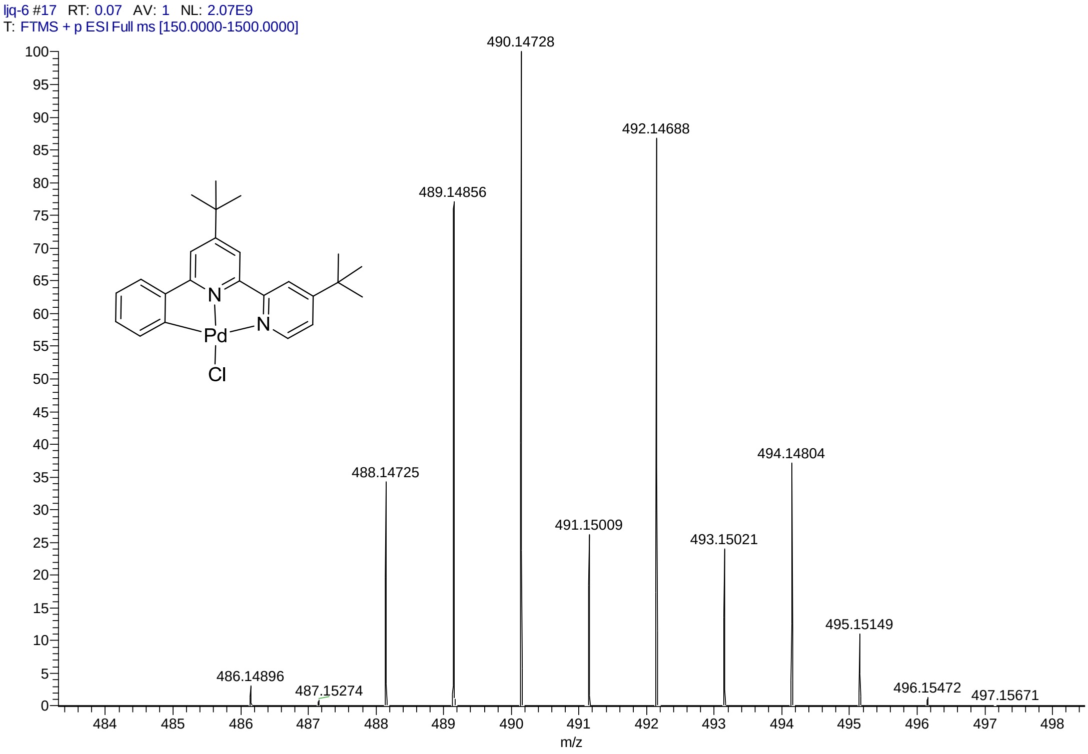

Figure S19. The HR-MS spectrum of **S8**.

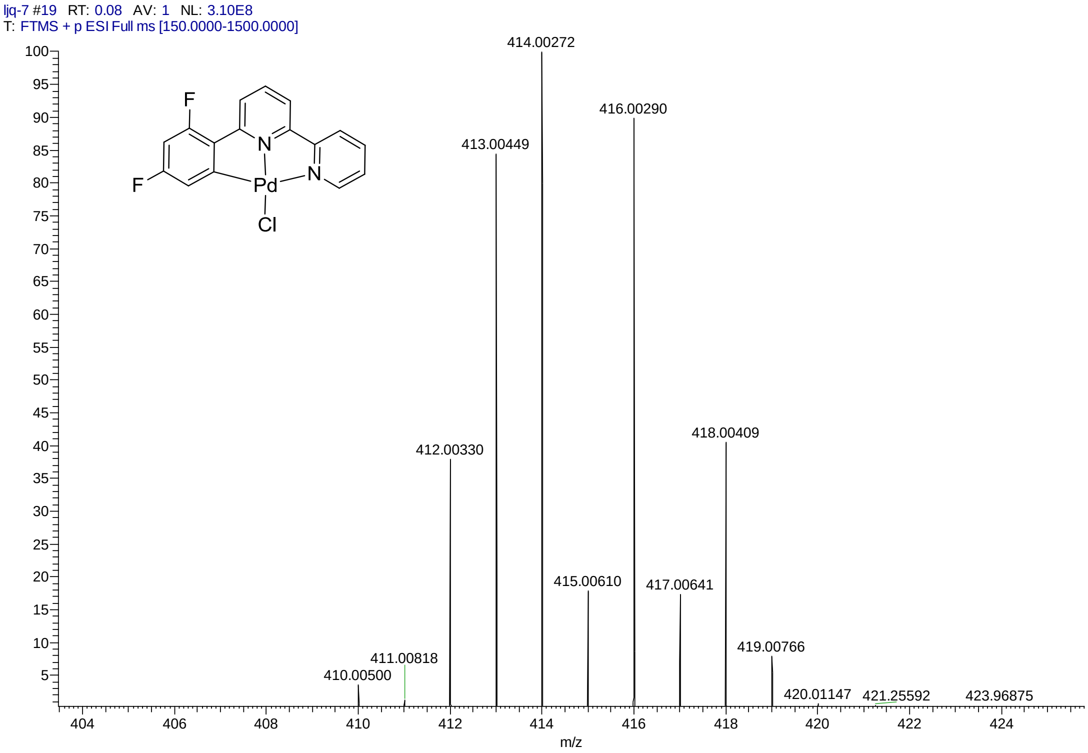

Figure S20. The HR-MS spectrum of **S10**.

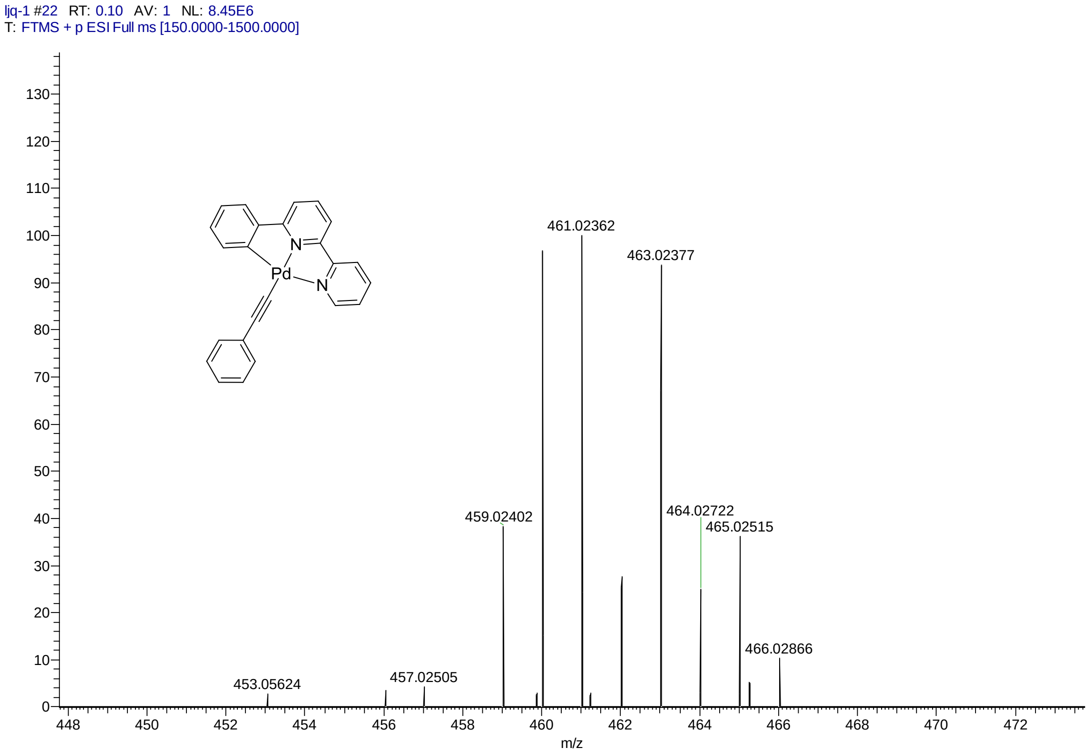

Figure S21. The HR-MS spectrum of **1**.

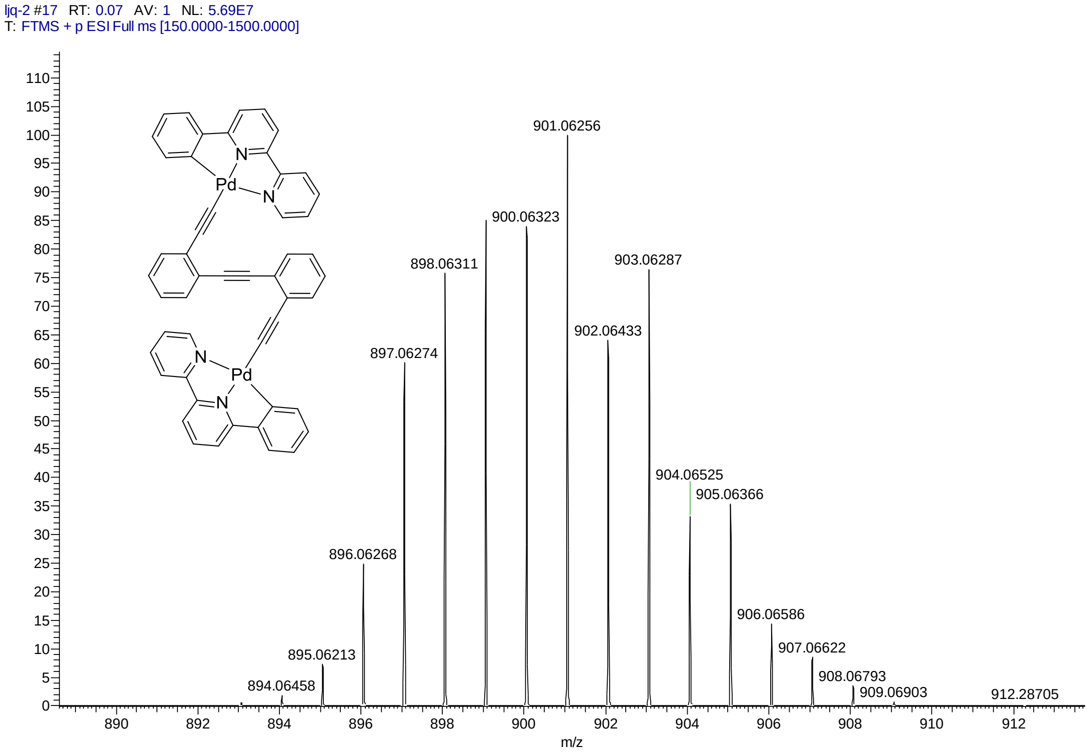

Figure S22. The HR-MS spectrum of **2**.

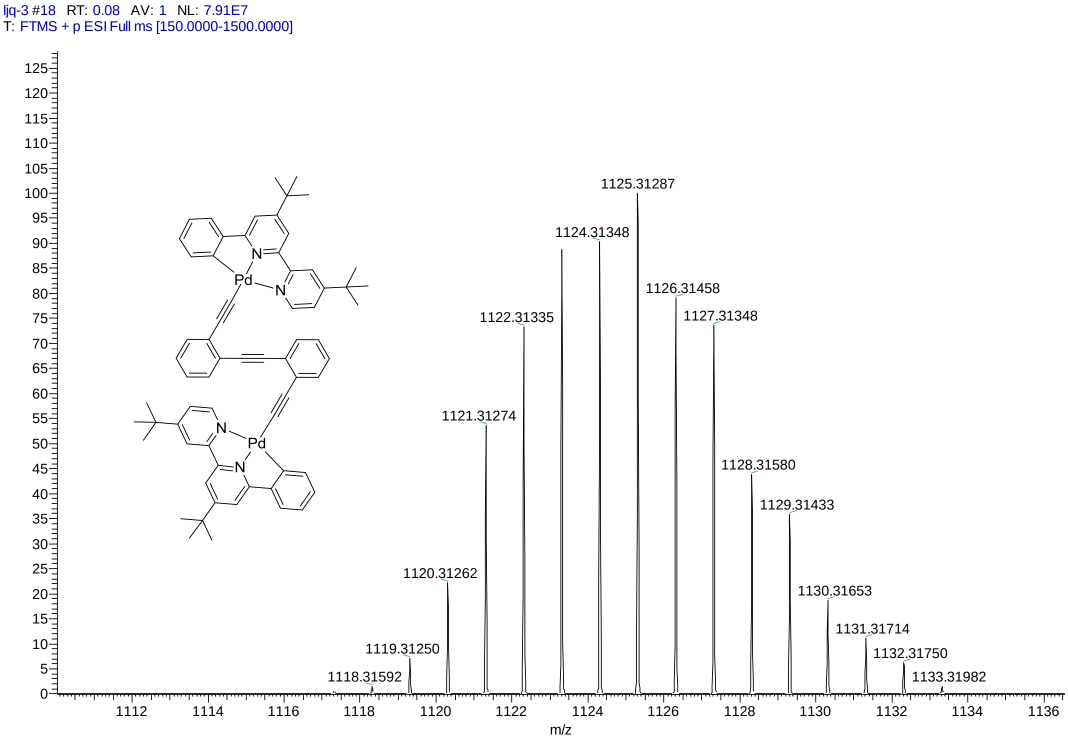

Figure S23. The HR-MS spectrum of **3**.

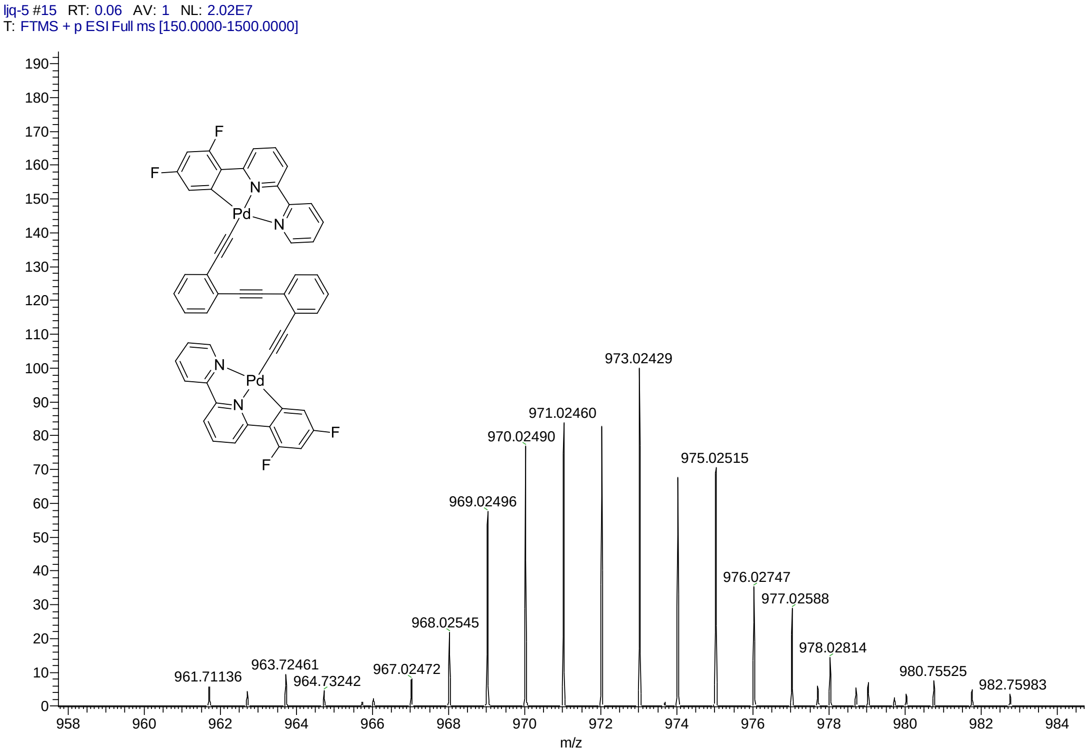

Figure S24. The HR-MS spectrum of **4**.

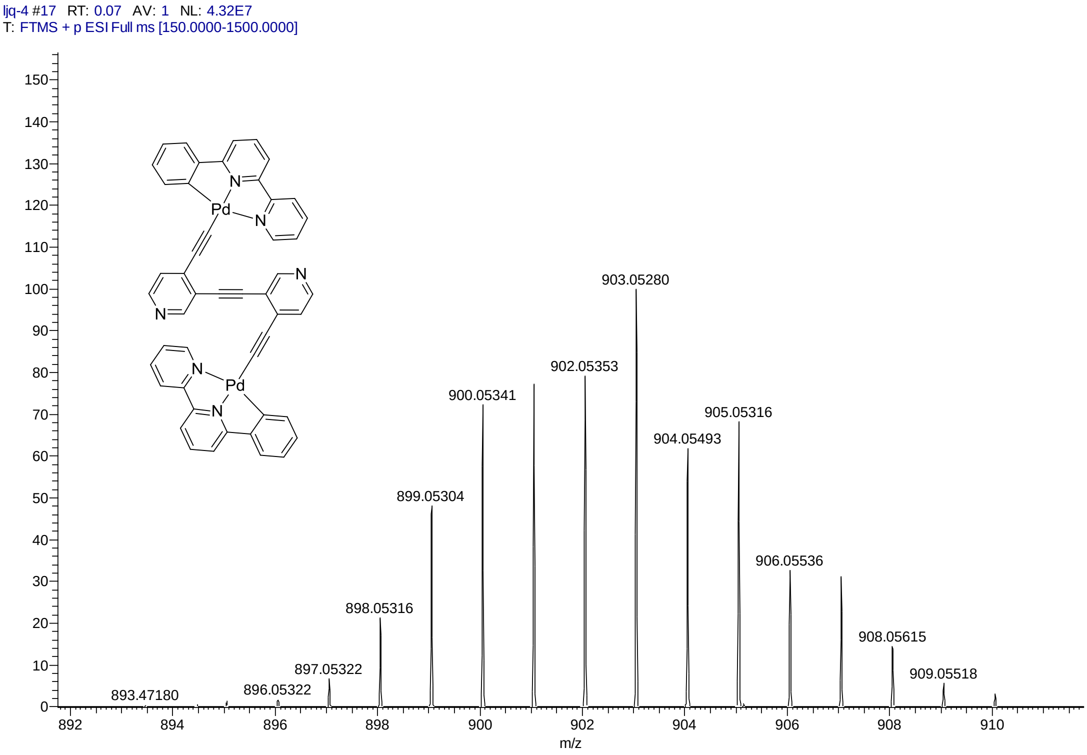

Figure S25. The HR-MS spectrum of **5**.

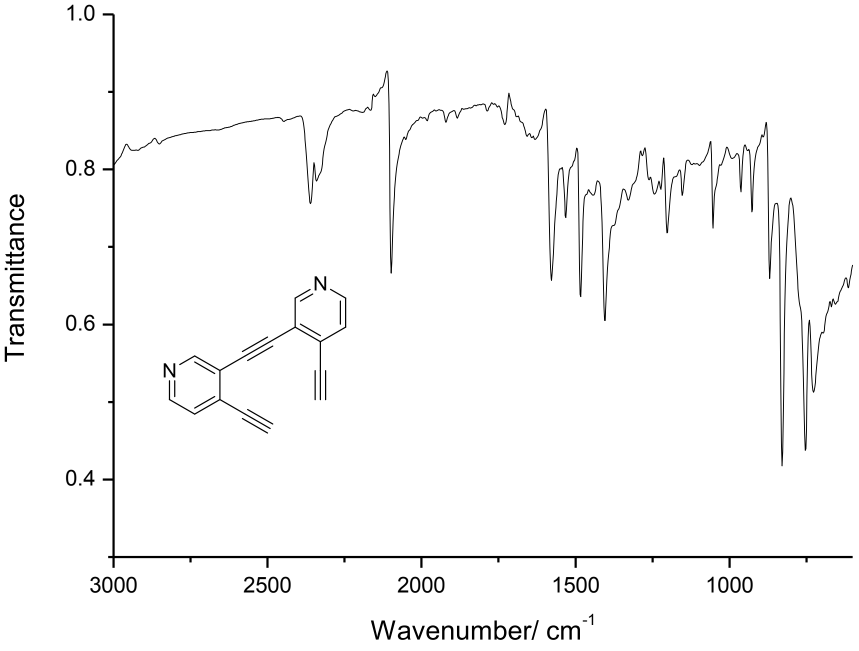

Figure S26. The IR spectrum of **S4**.

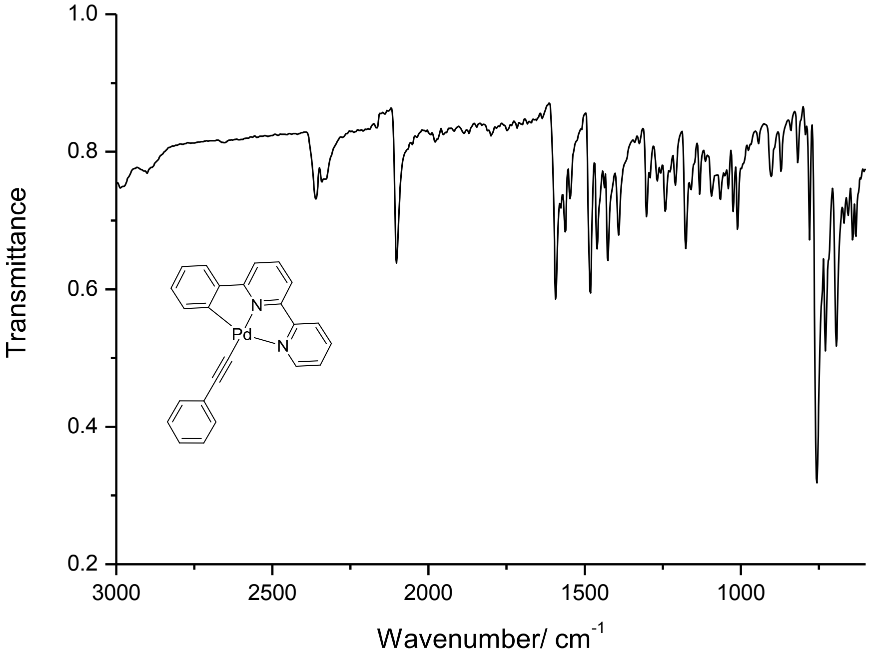

Figure S27. The IR spectrum of **1**.

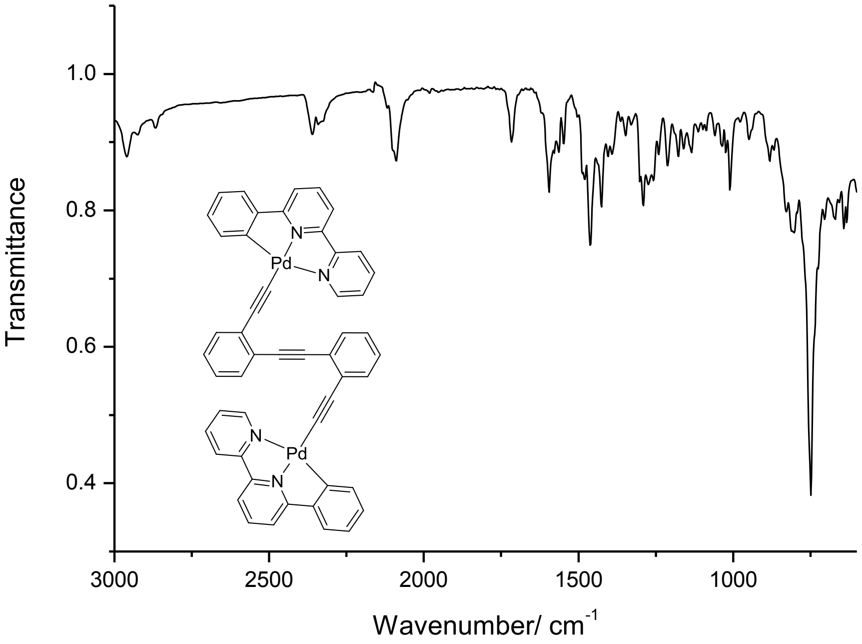

Figure S28. The IR spectrum of **2**.

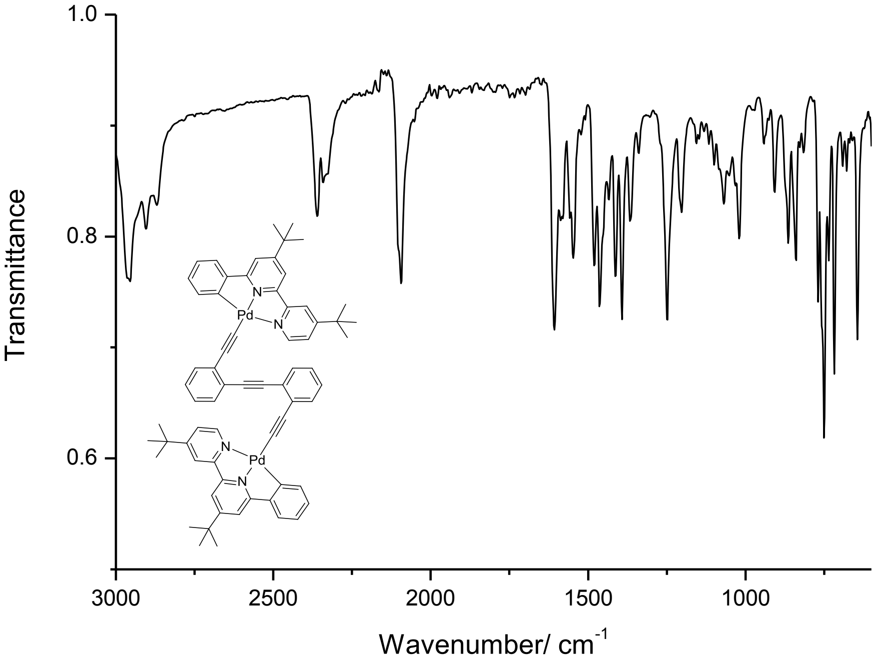

Figure S29. The IR spectrum of **3**.

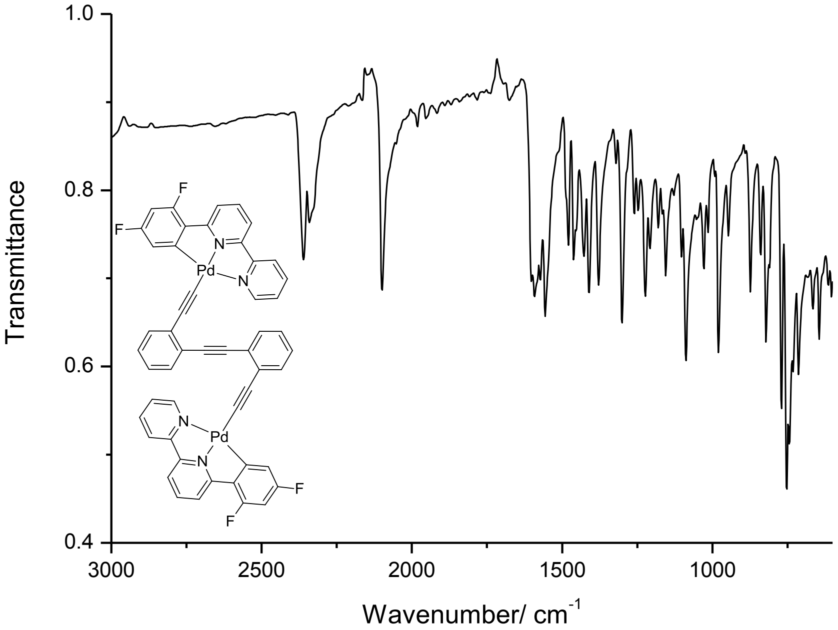

Figure S30. The IR spectrum of **4**.

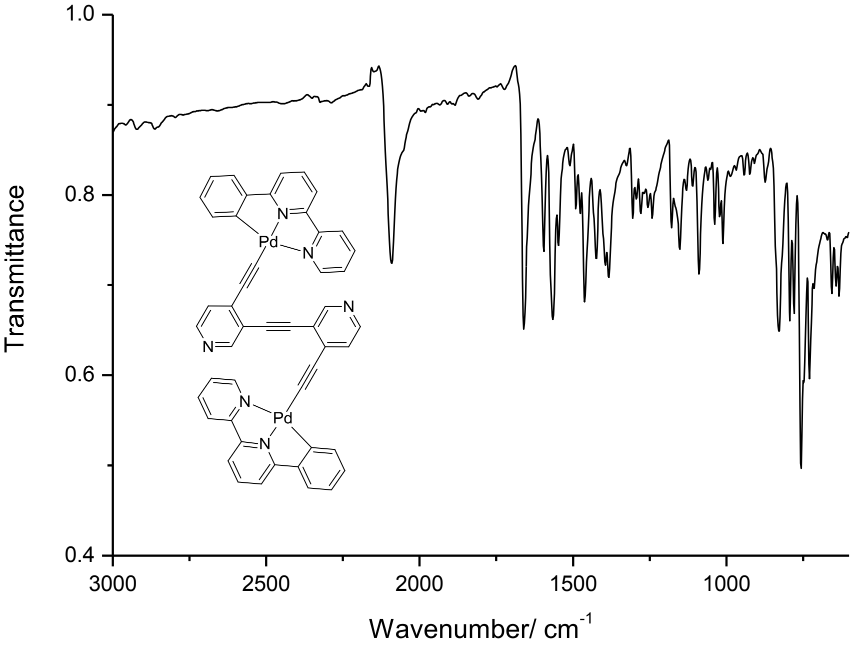

Figure S31. The IR spectrum of **5**.

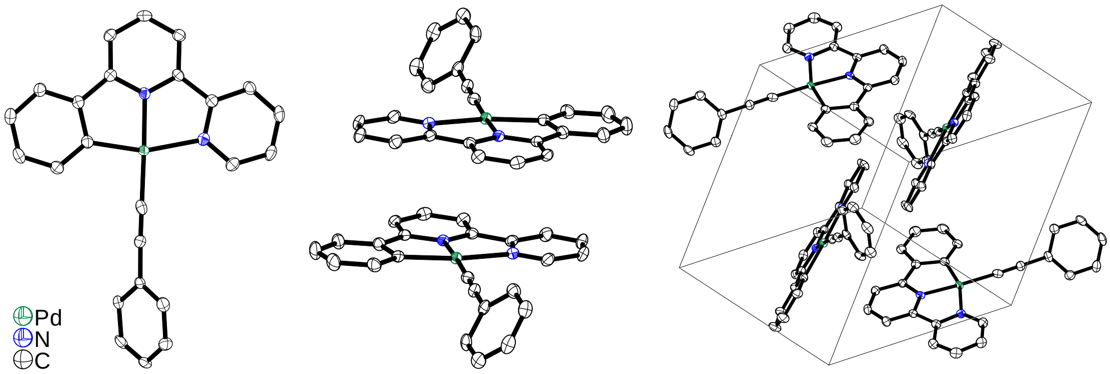

Figure S32. ORTEP plots and packing diagrams of the complex molecules in single crystals **1**.

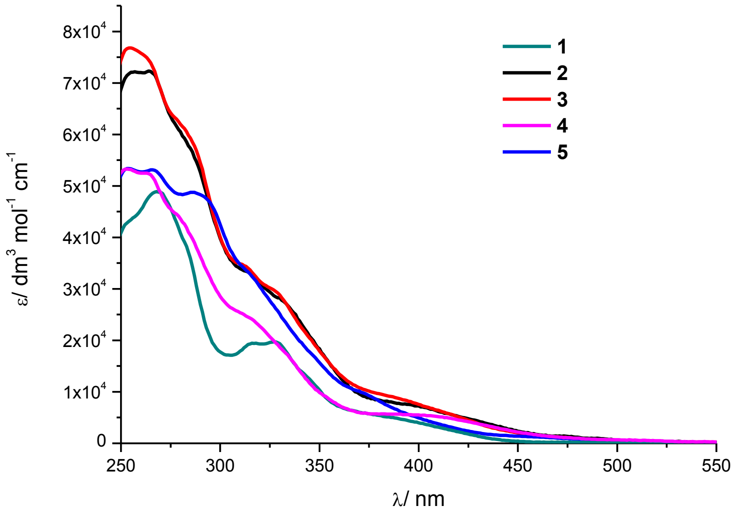

Figure S33. Absorption spectra of **1–5** (1×10^{-5} mol dm^{-3} in dichloromethane) at 298 K.

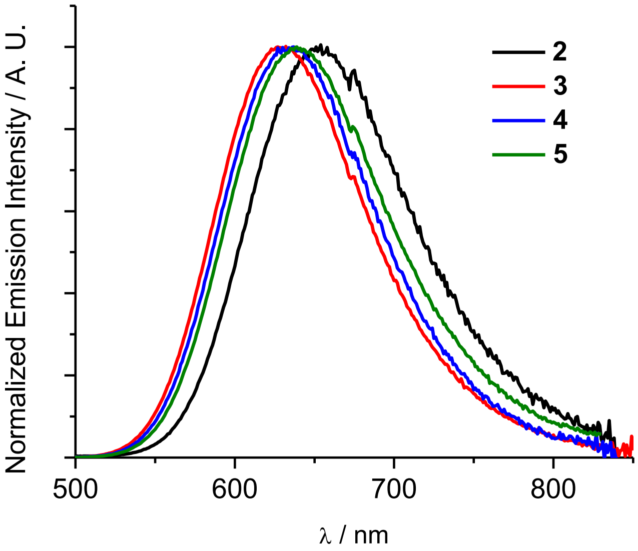

Figure S34. Normalized emission spectra of **2–5** in deoxygenated CH_2Cl_2 solutions (concentration ~1×10^{-5} mol dm^{-3}) at 298 K.

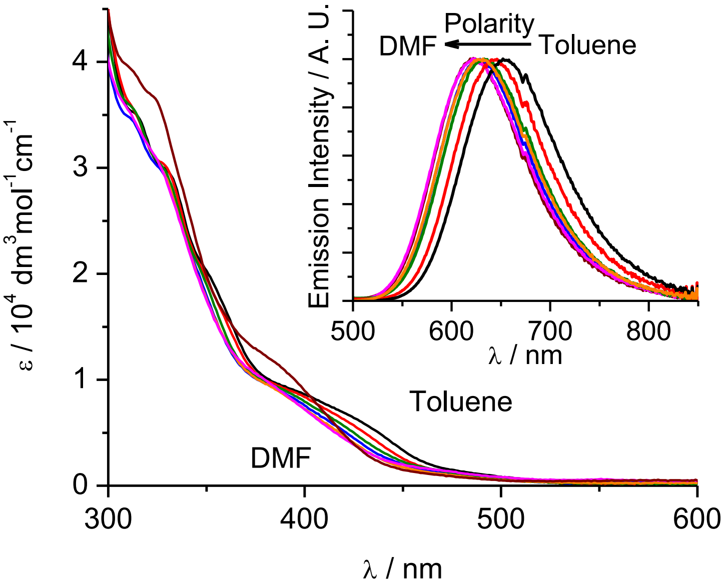

Figure S35. Absorption and normalized emission spectra of **3** in a variety of solvents with different polarities (DMF, acetonitrile, acetone, CH_2Cl_2, $CHCl_3$, 2-methyl-tetrahydrofuran, toluene).

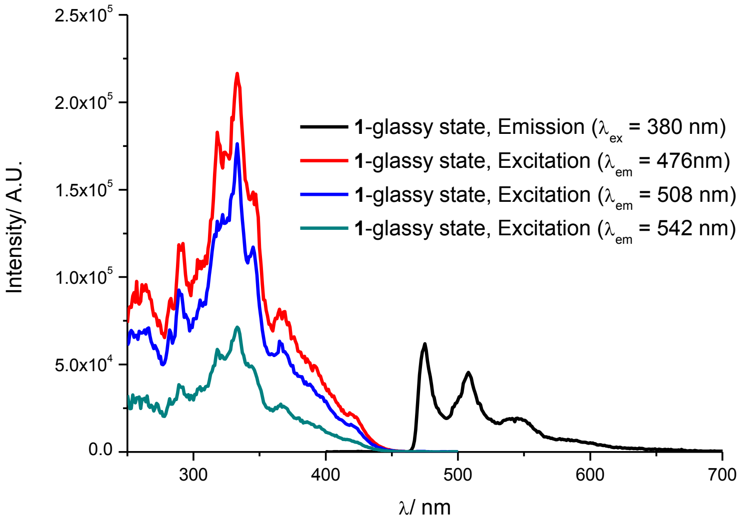

Figure S36. Glassy state emission and excitation spectra of **1** (1×10^{-5} mol dm^{-3} in 2-methyltetrahydrofuran) at 77 K.

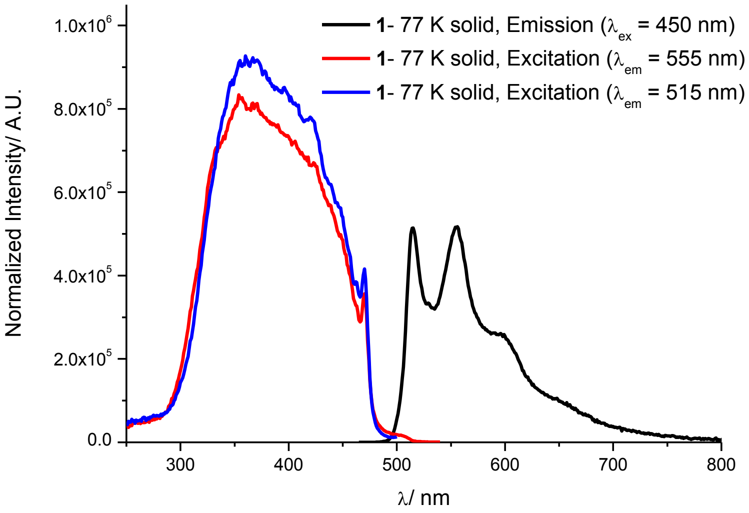

Figure S37. Solid-state emission and excitation spectra of **1** at 77 K.

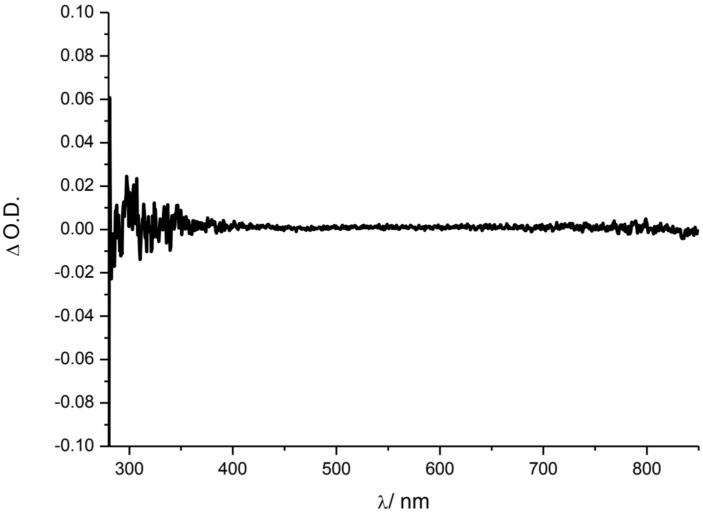

Figure S38. Nanosecond transient absorption spectrum of **1** in deoxygenated CH_2Cl_2 (2×10^{-4} mol dm^{-3}) solution at 298 K.

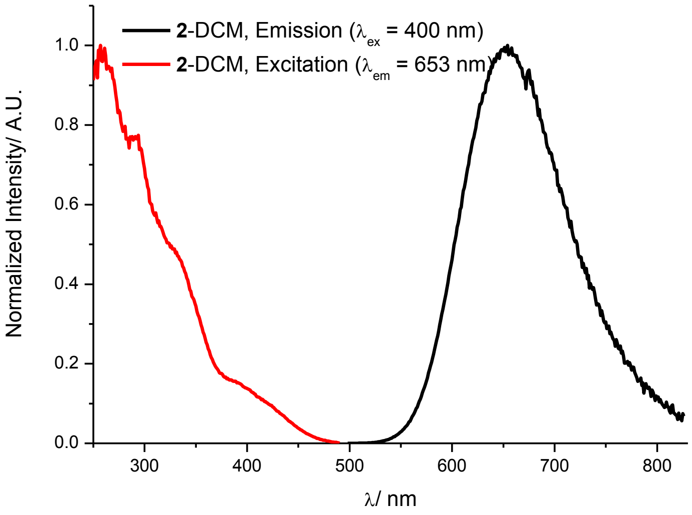

Figure S39. Solution-state emission and excitation spectra of **2** (1×10^{-5} mol dm^{-3} in deoxygenated CH_2Cl_2) at 298 K.

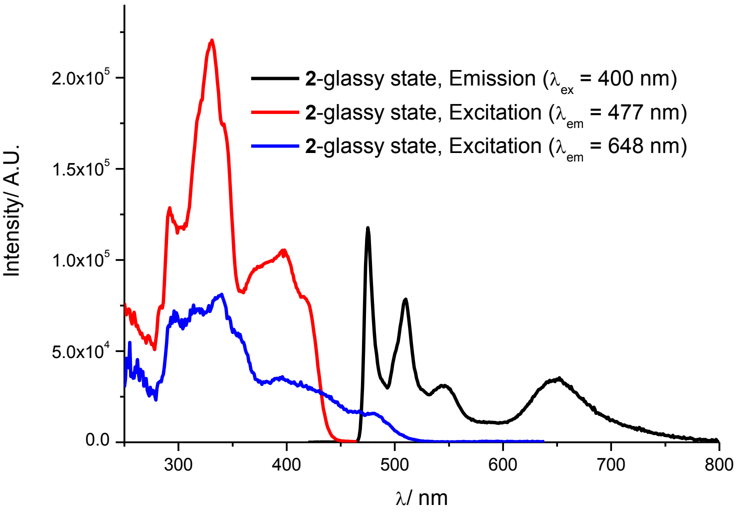

Figure S40. Glassy state emission and excitation spectra of **2** (1×10^{-5} mol dm^{-3} in 2-methyltetrahydrofuran) at 77 K.

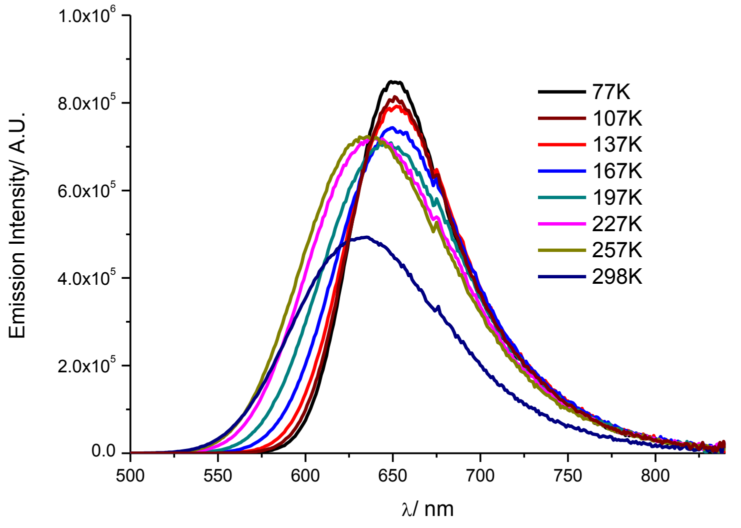

Figure S41. Temperature dependent (77–298 K) solid-state emission spectra of **2** (λ_{ex} = 400 nm).

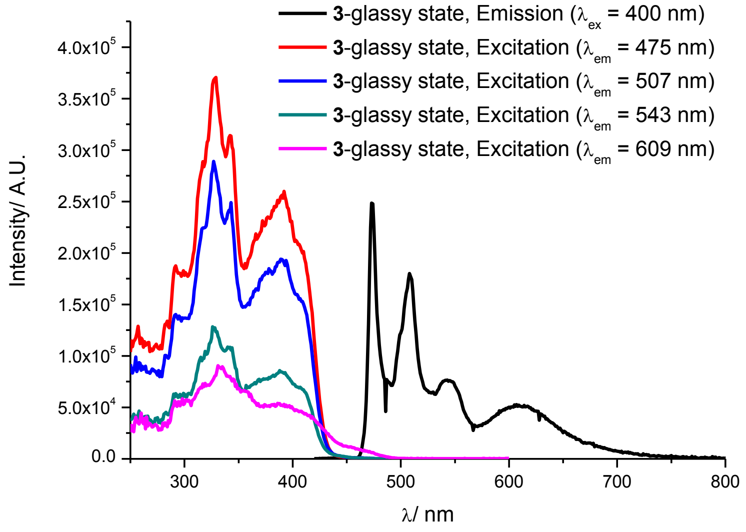

Figure S42. Glassy state emission and excitation spectra of **3** (1×10^{-5} mol dm^{-3} in 2-methyltetrahydrofuran) at 77 K.

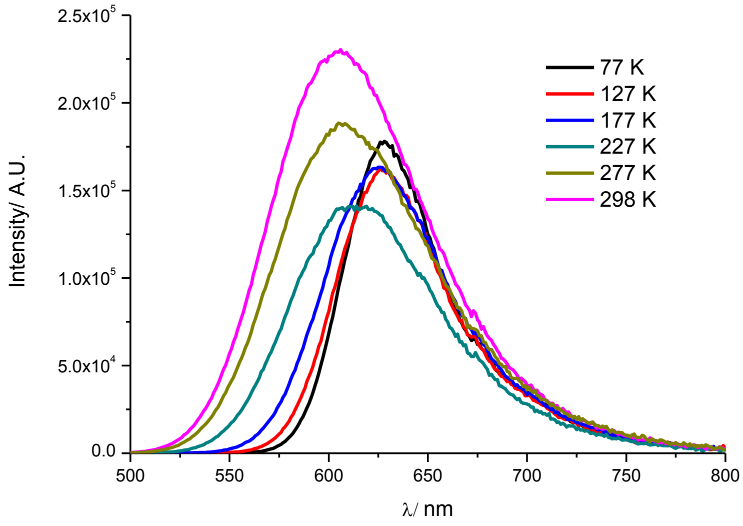

Figure S43. Temperature dependent (77–298 K) solid-state emission spectra of **3** (λ_{ex} = 400 nm).

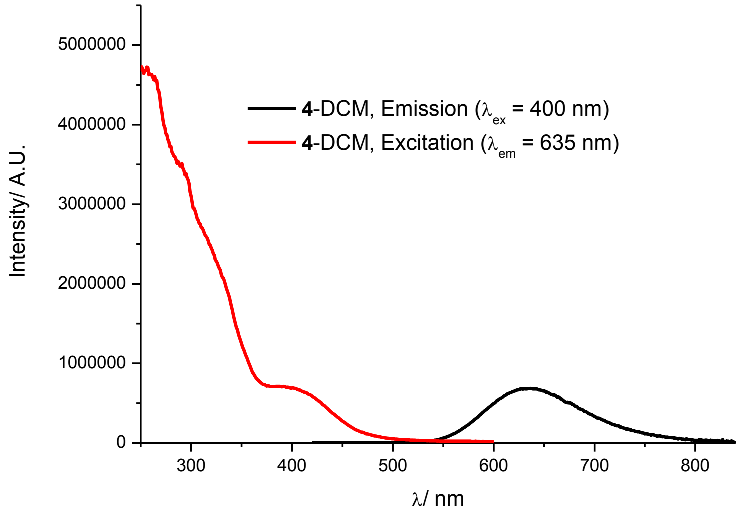

Figure S44. Solution-state emission and excitation spectra of **4** (1×10^{-5} mol dm^{-3} in deoxygenated CH_2Cl_2) at 298 K.

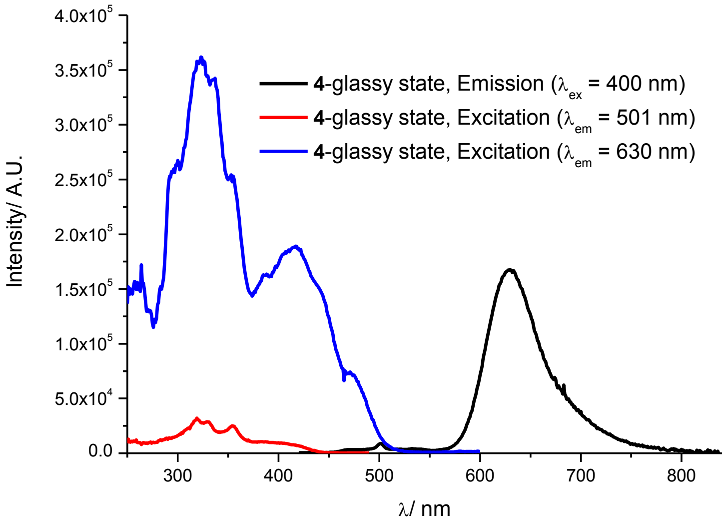

Figure S45. Glassy state emission and excitation spectra of **4** (1×10^{-5} mol dm^{-3} in 2-methyltetrahydrofuran) at 77 K.

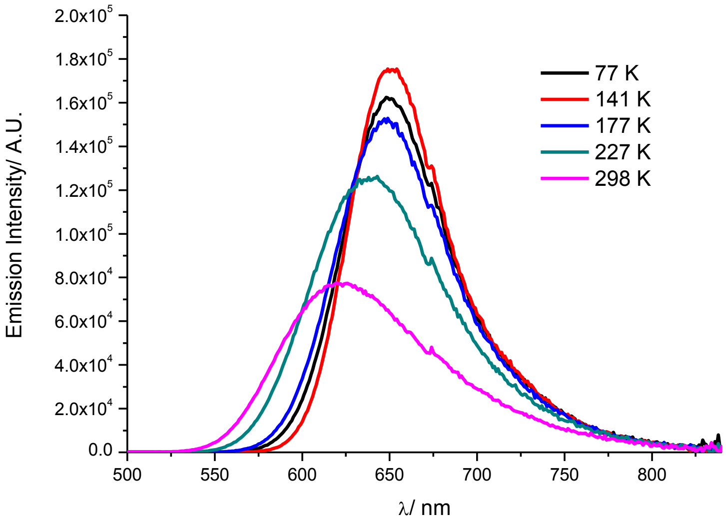

Figure S46. Temperature dependent (77–298 K) solid-state emission spectra of **4** (λ_{ex} = 400 nm).

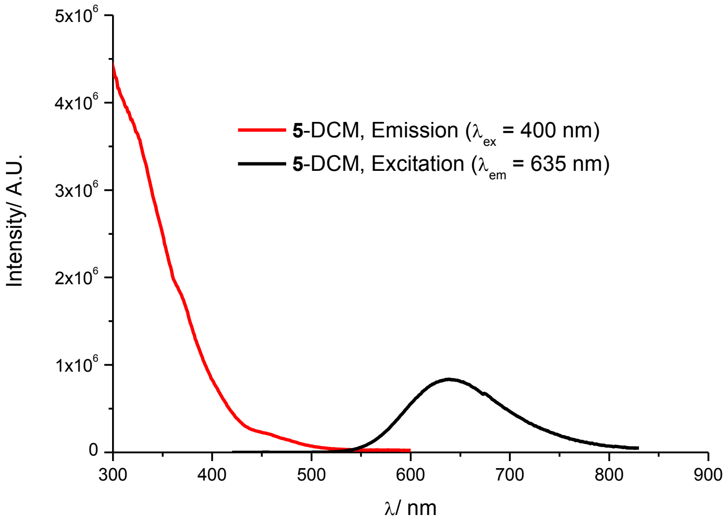

Figure S47. Solution-state emission and excitation spectra of **5** (1×10^{-5} mol dm^{-3} in deoxygenated CH_2Cl_2) at 298 K.

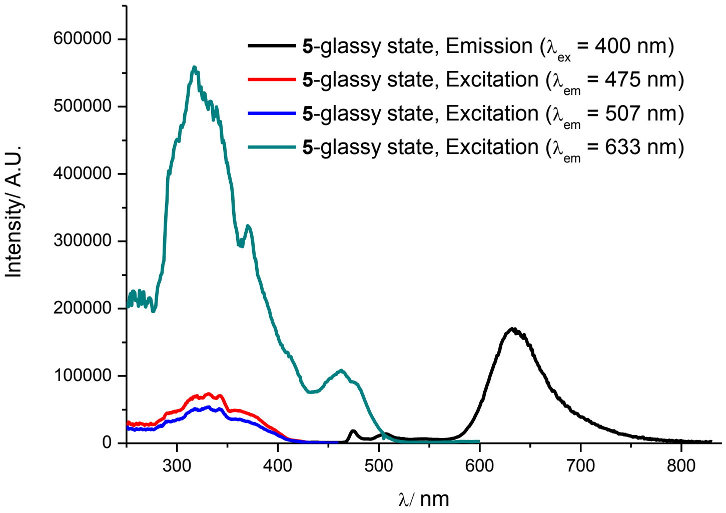

Figure S48. Glassy state emission and excitation spectra of **4** (1×10^{-5} mol dm^{-3} in 2-methyltetrahydrofuran) at 77 K.

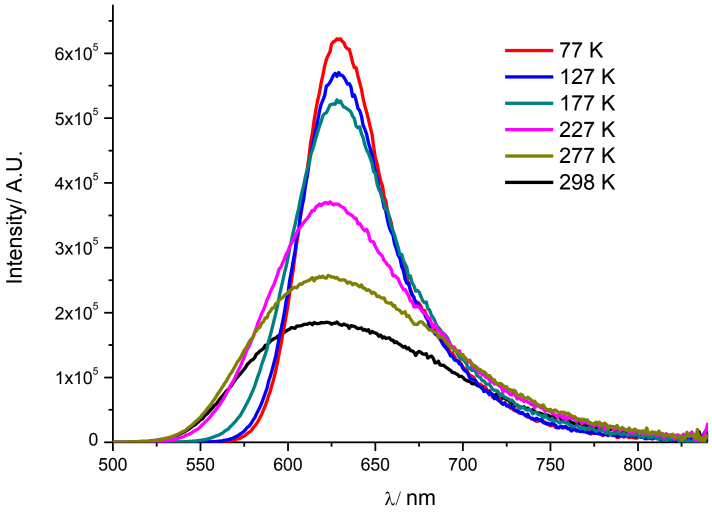

Figure S49. Temperature dependent (77–298 K) solid-state emission spectra of **5** (λ_{ex} = 400 nm).

Computational Results

All calculations were performed with Gaussian09 suite of program[4] employing density functional theory (DFT) and time-dependent density functional theory (TDDFT). The hybrid functional B3LYP[5] with dispersion correction (D3)[6] and double zeta basis set (LanL2DZ[7] for Pd and 6-31G(d)[8] for other atoms) was applied here. The geometries of complex **1** and both the folded conformations of complex **2** in ground state were full optimized based on the X-ray crystal structures. The singlet vertical excitation energy and corresponding electron transitions as well as the frontier molecular orbital analysis was based on the ground state geometry. Based on the excitation energy, $E_{n\rightarrow m}$, and oscillator strength f, the absorption spectra were simulated using Gaussian functions. A full-width at half-maximum (FWHM), that is, the broadening of each peak (individual transition) of 0.30 eV was applied. Solvent effects were considered using the Polarizable Continuum Model (PCM)[9] of SCRF procedure for dichloromethane, which was also employed experimentally. The geometries of folded conformation in the S_1, T_1 and T_2 states were fully optimized in a dichloromethane solution. According to the experimental results and the corresponding calculated absorption results, we suggest that the strongest phosphorescent emission of the folded conformation be assigned to the transition from T_2 to S_0.

Table S3. Calculated molecular orbitals of complex **1** and both the unfolded and folded conformations of complex **2** in CH_2Cl_2.

	MO	Energy / eV	Assignment
Complex **1**	L+5	–0.167	99% pπ+pπ*
	L+4	–0.318	11% Pd-dx^2-y^2 + 69% pπ*+σ*
	L+3	–0.571	28% Pd-dx^2-y^2 + 50% pπ*+σ*
	L+2	–1.128	98% pπ+pπ*
	L+1	–1.707	99% pπ+pπ*
	LUMO	–2.265	98% pπ+pπ*
	HOMO	–5.418	5% Pd-dxy + 95% pπ+pπ*
	H-1	–5.961	13% Pd-dxz + 85% pπ+pπ*
	H-2	–6.019	20% Pd-dyz + 78% pπ+pπ*
	H-3	**–6.276**	60% **Pd-dz^2** + 35% Pd-s
	H-4	–6.560	6% Pd-dyz + 82% pπ+pπ*
	H-5	–6.739	98% pπ+pπ*
Complex **2** (folded)	L+5	–0.914	96% pπ+pπ*
	L+4	–1.219	98% pπ+pπ*
	L+3	–1.345	98% pπ+pπ*
	L+2	–1.747	99% pπ+pπ*
	L+1	–1.885	98% pπ+pπ*
	LUMO	–2.234	99% pπ+pπ*
	HOMO	–5.200	18% Pd-dxz + 80% pπ+pπ*
	H-1	–5.464	17% Pd-dxz + 82% pπ+pπ*
	H-2	**–5.557**	78% **Pd-dz^2** + 19% Pd-s
	H-3	–5.892	14% Pd-dx^2-y^2 + 11% Pd-dyz + 70% pπ+pπ*
	H-4	–5.908	16% Pd-dx^2-y^2 + 8% Pd-dxz + 72% pπ+pπ*
	H-5	–5.998	10% Pd-dz^2 + 4% Pd-dx^2-y^2 + 6% Pd-dyz + 78% pπ+pπ*
	H-6	–6.122	4% Pd-dxz + 92% pπ+pπ*

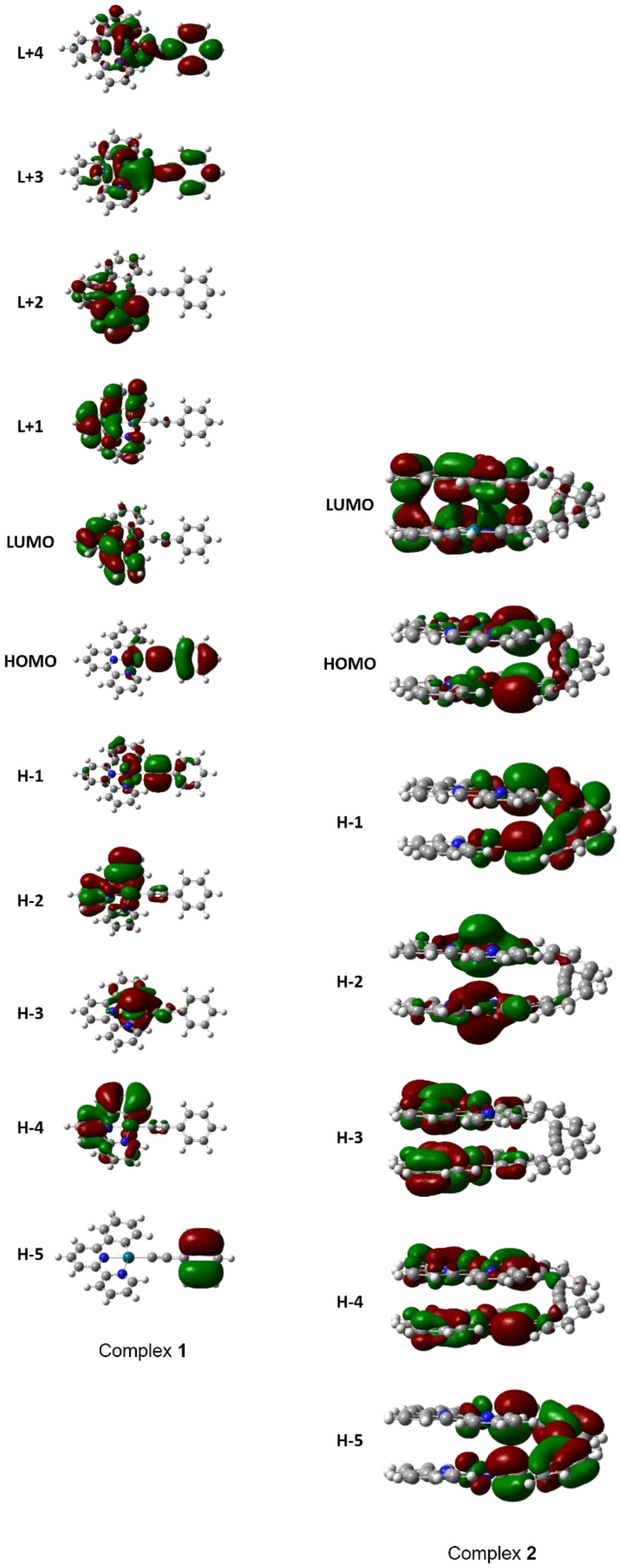

Complex **1**

Complex **2**

Figure S50. Calculated molecular orbitals of complex **1** and folded conformations of complex **2** in CH_2Cl_2.

Table S4. Structural parameters of optimized $\mathbf{S_0}$, $\mathbf{S_1}$, $\mathbf{T_1}$, and $\mathbf{T_2}$ state of **2**.

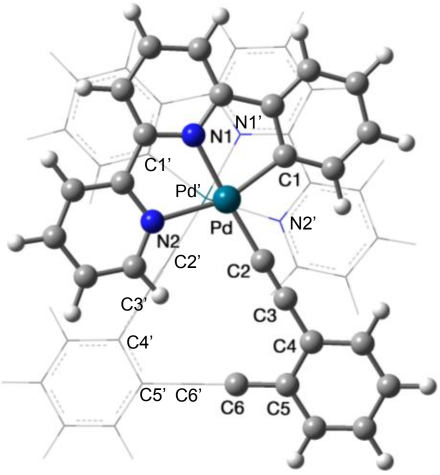

		$\mathbf{S_0}$	$\mathbf{S_1}$	$\mathbf{T_1}$	$\mathbf{T_2}$
Bond Distance (Å)	Pd–Pd’	3.34	2.86	3.04	2.85
	Pd–N1	2.03	2.02	2.02	2.02
	Pd–N2	2.18	2.19	2.19	2.19
	Pd–C1	1.99	2.01	2.00	2.00
	Pd–C2	1.96	1.97	1.95	1.97
	C2–C3	1.23	1.23	1.24	1.23
	C3–C4	1.42	1.41	1.40	1.41
Bond Angle (^{o})	Pd–C2–C3	172.2	176.6	175.0	176.1
	C2–C3–C4	175.5	179.2	179.4	179.3
Dihedral Angle (^{o})	C2–C3–C4–C5	70.3	89.9	67.4	85.9
	C2’–C3’–C4’–C5’	70.4	91.1	66.4	86.0
	C3–C4–C5–C6	3.0	1.5	6.8	1.8
	C3’–C4’–C5’–C6’	3.0	1.4	6.8	1.8
	N1–Pd–Pd’–N1’	65.4	57.9	59.4	58.3

Table S5. Calculated absorption properties of complex **1** and the folded conformations of complex **2** in CH_2Cl_2.

	Wavelength / nm	Oscillator Strength	Transition Configuration
Complex **1**	476.8	0.039	H → L
	407.9	0.037	H-1 → L
	388.3	0.031	H → L+1
	336.5	0.118	H-2 → L+1
Complex **2** (folded)	520.0	0.005	H → L
	478.2	0.067	H-2 → L
	465.8	0.023	H-1 → L

Table S6. Calculated emission properties of the folded conformations of complex **2** in CH_2Cl_2.

		Wavelength / nm	Oscillator Strength	Transition
Singlet	S_1-S_0	520.2	0.008	L → H
	S_2-S_0	481.2	0.038	L → H-2
	S_3-S_0	467.4	0.105	L → H-1
Triplet	T_1-S_0	700.1	----	L → H
	T_2-S_0	602.5	----	L → H-1

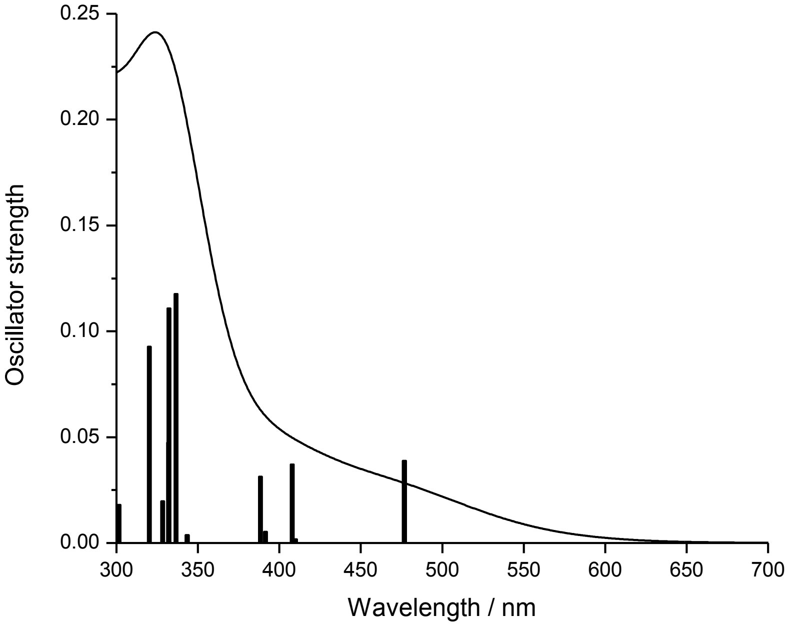

Figure S51. Calculated absorption spectrum of complex **1** in CH_2Cl_2.

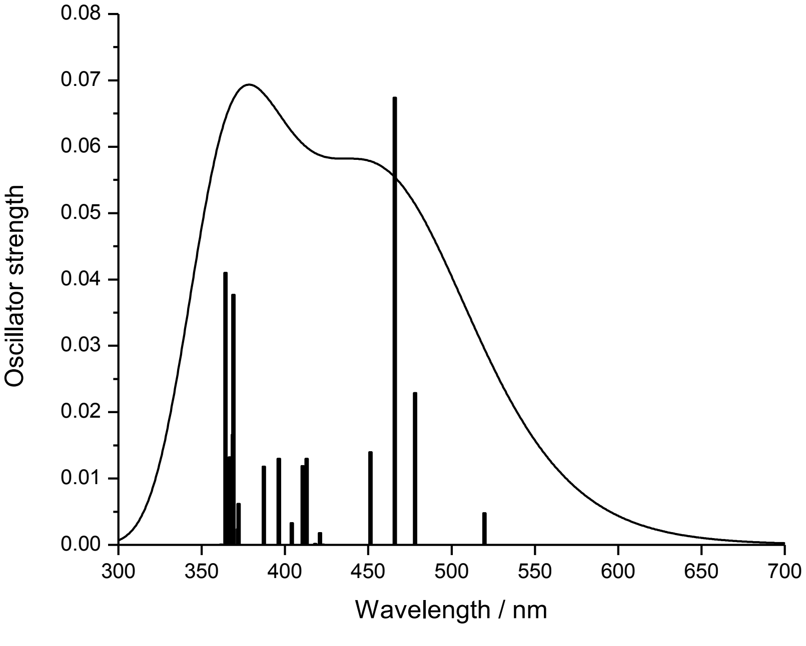

Figure S52. Calculated absorption spectrum of the folded conformation of complex **2** in CH_2Cl_2.

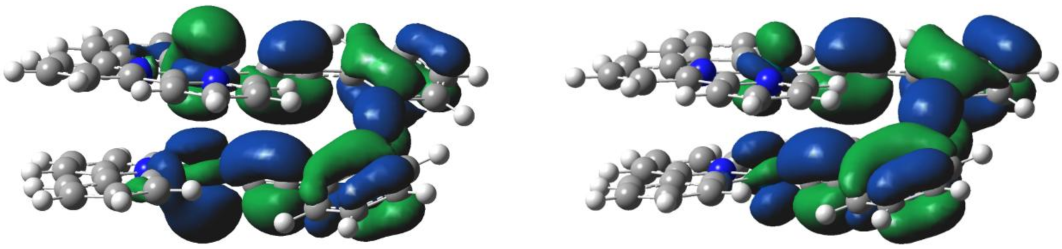

T2 **T1**

Figure S53. One-electron spin density on the optimized **T2** (left) and **T1** (right) state of complex **2**, calculated by TD-DFT close-shell model.

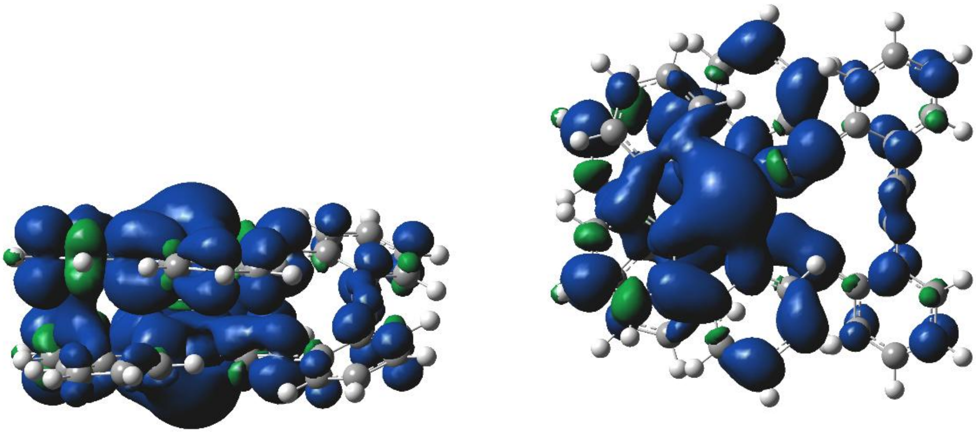

Side view **Top view**

Figure S54. Triplet two-electron spin density on the optimized **T1** state of complex **2**, calculated by UDFT open-shell model.

References

1. R. Diercks and K. P. C. Vollhardt, *Angew. Chem. Int. Ed.*, 1986, **25**, 266.
2. G. Chelucci, S. Baldino, G. A. Pinna and B. Sechi, *Tetrahedron Lett.*, 2008, **49**, 2839.
3. C. Zou, J. Q. Lin, S. Suo, M. Xie, X. Y. Chang and W. Lu, *Chem. Commun*., 2018, **54**, 5319.
4. M. J. Frisch, H. B. Schlegel, G. E. Scuseria, M. A. Robb, J. R. Cheeseman, G. Scalmani, V. Barone, B. Mennucci, G. A. Petersson, H. Nakatsuji, M. Caricato, X. Li, H. P. Hratchian, A. F. Izmaylov, J. Bloino, G. Zheng, J. L. Sonnenberg, M. Hada, M. Ehara, K. Toyota, R. Fukuda, J. Hasegawa, M. Ishida, T. Nakajima, Y. Honda, O. Kitao, H. Nakai, T. Vreven, J. A. Montgomery, Jr., J. E. Peralta, F. Ogliaro, M. Bearpark, J. J. Heyd, E. Brothers, K. N. Kudin, V. N. Staroverov, R. Kobayashi, J. Normand, K. Raghavachari, A. Rendell, J. C. Burant, S. S. Iyengar, J. Tomasi, M. Cossi, N. Rega, J. M. Millam, M. Klene, J. E. Knox, J. B. Cross, V. Bakken, C. Adamo, J. Jaramillo, R. Gomperts, R. E. Stratmann, O. Yazyev, A. J. Austin, R. Cammi, C. Pomelli, J. W. Ochterski, R. L. Martin, K. Morokuma, V. G. Zakrzewski, G. A. Voth, P. Salvador, J. J. Dannenberg, S. Dapprich, A. D. Daniels, Ö. Farkas, J. B. Foresman, J. V. Ortiz, J. Cioslowski and D. J. Fox, *Gaussian, Inc., Wallingford CT*, 2009.
5. A. D. Becke, *J. Chem. Phys.*, 1993, **98**, 5648.
6. S. Grimme, J. Antony, S. Ehrlich, H. A. Krieg, *J. Chem. Phys.*, 2010, **132**, 154104.
7. C. E. Check, T. O. Faust, J. M. Bailey, B. J. Wright, T. M. Gilbert and L. S. Sunderlin, *J. Phys. Chem. A*, 2001, **105**, 8111.
8. P. C. Hariharan and J. A. Pople, *Theoretica Chimica Acta*, 1973, **28**, 213.
9. V. Barone and M. Cossi, *J. Phys. Chem. A*, 1998, **102**, 1995.